UCLA

Title
Two-photon calcium imaging of neuronal activity

Authors
Grienberger, Christine
Giovannucci, Andrea
Zeiger, William
et al.

Two-photon calcium imaging of neuronal activity

Christine Grienberger [1], Andrea Giovannucci [2,3], William Zeiger [4] and Carlos Portera-Cailliau [4,5] ✉

Abstract | In vivo two-photon calcium imaging (2PCI) is a technique used for recording neuronal activity in the intact brain. It is based on the principle that, when neurons fire action potentials, intracellular calcium levels rise, which can be detected using fluorescent molecules that bind to calcium. This Primer is designed for scientists who are considering embarking on experiments with 2PCI. We provide the reader with a background on the basic concepts behind calcium imaging and on the reasons why 2PCI is an increasingly powerful and versatile technique in neuroscience. The Primer explains the different steps involved in experiments with 2PCI, provides examples of what ideal preparations should look like and explains how data are analysed. We also discuss some of the current limitations of the technique, and the types of solutions to circumvent them. Finally, we conclude by anticipating what the future of 2PCI might look like, emphasizing some of the analysis pipelines that are being developed and international efforts for data sharing.

Understanding how neurons communicate with each other to generate movements, emotions or cognition is a central goal of neuroscience, requiring tools to record neuronal activity. For most of the twentieth century, electrophysiology was the only method available to neuroscientists to record neural activity. Although electrophysiology remains the gold standard to accurately record action potentials and sub-threshold changes in membrane potential, it suffers from important shortcomings. Electrodes must be inserted into brain tissue, which causes trauma and, potentially, triggers irritability of neurons. Furthermore, the number of neurons that can be recorded simultaneously is limited, and their identity cannot be readily identified — neurons are almost always targeted blindly, and therefore there is a bias towards very active neurons. Recent advances in silicon probe technology, which now allow for multiple probes to be inserted into the brain (each with hundreds of contact sites), have expanded the number of neurons and brain regions that can be sampled with electrophysiology, but with greater invasiveness, higher cost and the same limitations compared with single-neuron electrode recordings.

Optical probing of neural activity, especially calcium imaging, has become a popular alternative to electrophysiology. Recording neural activity with fluorescence probes — primarily calcium and voltage sensors — has become mainstream in neuroscience[1,2]. In particular, calcium imaging with two-photon (2P) microscopy has become the preferred method for recording neuronal ensemble dynamics in the intact brain over the past

two decades[3,4], because it offers several advantages over in vivo electrophysiology.

Principles of calcium imaging
The ability to conduct calcium imaging experiments with rigour and reproducibility requires an in-depth knowledge of what signal is being measured and how. This requires, in turn, a basic understanding of the experimental techniques and equipment necessary to detect that signal, and of the computational pipelines to analyse and interpret the signal. In general terms, calcium imaging relies on the detection of changes in intracellular calcium concentration ($[Ca^{2+}]_i$) using fluorescent calcium indicators. Calcium contributes to a range of complex signals within neurons, from triggering neurotransmitter release to long-lasting synaptic plasticity in dendritic branches and spines. Importantly, the $[Ca^{2+}]_i$ regulates these processes over vastly different timescales, from a few microseconds to several hours. Thus, the time course, the amplitude or the site of its action in distinct cellular compartments are all essential determinants for the function of intraneuronal calcium signals. However, when discussing calcium imaging as a means of probing neural activity, which is the principal focus of this Primer, we are referring to Ca^{2+} ions entering the cell body (the soma) through voltage-gated calcium channels when a neuron fires an action potential (FIG. 1a). Therefore, because the $[Ca^{2+}]_i$ in the soma correlates with action potential firing, somatic calcium imaging is an indirect way of assessing a neuron's level of activity. Ca^{2+} ions can also enter neurons through other

[1]Department of Biology and Volen National Center for Complex Systems, Brandeis University, Waltham, MA, USA.

[2]Joint Department of Biomedical Engineering University of North Carolina at Chapel Hill and North Carolina State University, Chapel Hill, NC, USA.

[3]UNC Neuroscience Center, University of North Carolina at Chapel Hill, Chapel Hill, NC, USA.

[4]Department of Neurology, David Geffen School of Medicine at UCLA, Los Angeles, CA, USA.

[5]Department of Neurobiology, David Geffen School of Medicine at UCLA, Los Angeles, CA, USA.

✉e-mail: cpcailliau@mednet.ucla.edu

https://doi.org/10.1038/s43586-022-00147-1

channels (such as NMDA receptors) and may be highly localized to specific domains, such as dendritic spines and axon boutons. Although not described in detail within this Primer, the general principles of somatic calcium imaging can be readily applied to probe these subcellular compartments.

The goal of calcium imaging is to generate a calcium trace that reflects changes in fluorescence intensity of the calcium indicator. Many studies that conducted simultaneous calcium imaging and electrode recordings in single neurons have shown that somatic calcium signals can be used to infer the underlying action potential firing[5] (FIG. 1b). In principle, any fluorescence microscope can be used to detect changes in indicator fluorescence intensity related to neuronal activity. This Primer focuses on the use of 2P microscopy because it is ideally suited for in vivo calcium imaging experiments in highly scattering tissue, such as the brain.

There are three major steps involved in two-photon calcium imaging (2PCI) experiments that we review in this Primer (FIG. 1c): expressing or loading the calcium indicator; visualizing changes in fluorescence intensity induced by neuronal activity; and extracting and analysing those signals. In this Primer, we expand on each of these steps to prepare the reader to embark on 2PCI experiments. In birds, rodents and non-human primates, it is necessary to remove the skull and implant a transparent optical element (typically a cranial window, or alternatively a prism or a different type of lens) in order to visualize changes in fluorescence intensity from genetically encoded calcium indicators (GECIs). 2PCI also

relies on specialized microscopes equipped with lasers to excite the GECI and photodetectors to quantify the emitted photons[6].

Advantages of 2PCI

There are several reasons why 2PCI has become so popular in neuroscience in the past decade, and they mostly have to do with key advances in biology, technology and computer science that collectively made 2PCI increasingly easier and cost-effective. Importantly, 2PCI also offers unique advantages over in vivo electrophysiology. First, 2PCI is less invasive because it does not generally require disrupting the dura or the underlying brain. Second, it can be combined with sophisticated genetic tools (for example, Cre–*loxP*, Flp/FRT, Tet-ON/OFF), which allows precise targeting and timing of expression within specific neuronal populations, and can readily estimate spatial relationships between neurons. Third, it is possible to use 2PCI to record activity in subcellular compartments (soma, dendrites, axons, even single spines or boutons), as well as signals from non-neuronal cells (microglia, astrocytes, vascular endothelium) that are not related to action potential firing. Fourth, 2PCI allows for longitudinal imaging of identified cells over weeks or months and over a larger spatial extent (multiple cortical areas).

There are other reasons why many laboratories around the world are doing 2PCI beyond its advantages over electrophysiology. First, it has become a lot cheaper to purchase commercial turnkey laser/microscope systems. Even the basic models include the
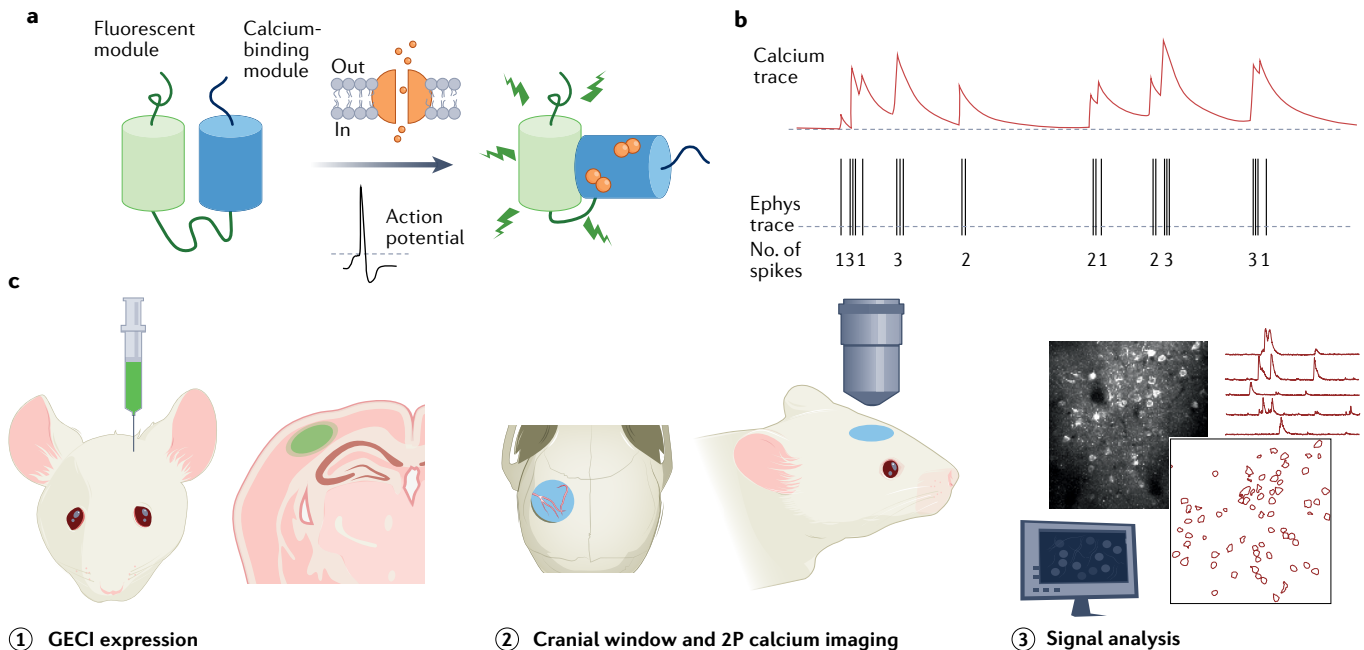

① GECI expression

② Cranial window and 2P calcium imaging

③ Signal analysis

Fig. 1 | **The principles of fluorescence calcium imaging. a** | Mechanism of calcium indicator function. A calcium sensor requires a calcium-binding element and a fluorescent molecule. Genetically encoded calcium indicators (GECIs) are combinations of two proteins, a calcium-binding protein and a fluorescent protein. Action potential firing leads to an influx of Ca^{2+} ions into the cell. Binding of Ca^{2+} to the calcium-sensing module causes a conformational change in the fluorescent molecule, which causes a change in its brightness. **b** | Relationship between neural spiking and calcium traces. Owing to limitations in signal-to-noise ratio and in temporal resolution, calcium imaging cannot reliably detect individual spikes within trains of action potentials. **c** | Three steps in calcium imaging: introducing the calcium indicator via direct injection into the brain (step 1); implantation of a cranial window or optical fibre (not shown) to gain optical access into brain tissue and in vivo imaging of changes in fluorescence of the indicator with a two-photon (2P) microscope (step 2); and analysis of the fluorescence images and the extracted calcium traces (step 3).

latest technologies for fast scanning (resonant mirrors, piezo-moving objectives) and detection of emitted fluorescence (gallium arsenide photodetectors). High-end systems can be customized to include adaptive optics for deeper imaging, a separate laser module for optogenetics or spatio-temporal multiplexing for imaging at multiple locations or depths. Second, the dramatic improvements in GECIs — such as shorter rise times and better signal-to-noise ratio — have made it possible to extract spike rates with greater accuracy. The emergence of red-shifted indicators has extended 2PCI to deeper brain structures because red photons scatter less in deep tissue. For example, the use of a red GECI allowed 2PCI of CA1 pyramidal neurons at a depth of 1,000 μm in 4-week-old mice without removal of the overlying cortical tissue[7]. In parallel, the cornucopia of viral and transgenic tools allows researchers to easily target molecularly defined cell types or brain regions. Third, it is increasingly easy to process and analyse calcium signals with software packages for acquisition, as well as registration, segmentation, deconvolution and deep learning for spike inference. Finally, scientists find significant appeal in the flexibility of 2PCI. With the same general approach, one can record activity at the soma, dendrites or axons, in a seemingly endless array of preparations from zebrafish embryos or neonatal mice to adult mice performing behavioural tasks. The same 2P microscope can also help visualize disease-relevant pathogenic molecules (such as amyloid-β), markers of specific subtypes (interneuron subclasses and glia), blood flow, optogenetic proteins and neuronal structure (spines, boutons), among others. By contrast, silicon probes and tetrodes cannot ever offer such capabilities.

In this Primer, we provide an overview of the major steps involved in conducting 2PCI experiments and analysing the resulting data, providing examples of what optimal data should look like. We also discuss some of the limitations of 2PCI and provide an outlook of what the future holds for this remarkable methodology. Although the Primer is quite comprehensive and mentions a wide range of 2PCI applications, we have focused our discussion on 2PCI to record neuronal signals through glass cranial windows in mice because we feel this would be a good starting point for the average potential user. We do not discuss single-photon calcium imaging, including the use of miniaturized portable microscopes (also known as mini-scopes).

Experimentation
In this section, we review the major steps involved: choosing the most appropriate calcium indicator; introducing the indicator into the brain; implanting a cranial window to gain access to the cells expressing the indicator; using 2P microscopy for calcium imaging; and producing images. Throughout, we guide the reader through the entire process, pointing to available resources that make each step more accessible.

Types of calcium indicator
The first step in planning a 2PCI experiment is choosing a calcium indicator, which can be either chemical or genetically encoded (FIG. 2). Various factors go into

this decision, including experimental imaging preparation (acute versus chronic), cell type and intracellular compartment of interest and multiplexing with other fluorescent indicators or proteins, among others.

Chemical indicators. There are numerous chemical calcium indicators (for example, Fura-2, OGB-1, Indo-1, Fluo-4) (FIG. 2a), most of which are iterations of those originally designed in the early 1980s[8,9]. The specific properties of each have been reviewed extensively elsewhere[10]. The variety in chemical indicators is one of their major advantages, with indicators available in multiple colours, in ratiometric and non-ratiometric forms, and with a range of different dissociation constants (K_d) optimized for different cell types or intracellular compartments. The K_d corresponds to the $[Ca^{2+}]_i$ at which half of the indicator molecules are bound to Ca^{2+}. Deciding on whether to use an indicator with higher affinity (K_d of up to 200 nM) or lower affinity ($K_d > 200$–500 nM) should be guided by the scientific question. Fluorescent signals recorded with low-affinity indicators — which add little buffer capacity to the cell — reflect more accurately the change in the free cytosolic $[Ca^{2+}]$. These calcium signals will have faster rise and decay times than those recorded with high-affinity indicators[11]. However, the use of low-affinity calcium indicators is counterbalanced by the need for sufficient detection sensitivity. This problem becomes increasingly important, when imaging in noisy in vivo conditions and when recording from smaller neural processes, such as dendritic spines. In these conditions, higher-affinity indicators remain, despite their limitations, the indicators of choice. A major drawback of chemical indicators, however, is that after being loaded into cells, the indicator will diffuse out of cells over time and will no longer generate useful signals. As such, the use of chemical indicators is limited to acute surgical preparations and generally short (several hours) imaging timescales[12,13]. Because of these limitations, few 2PCI studies currently use chemical indicators.

Genetically encoded calcium indicators. The next major advance for calcium imaging was the discovery of green fluorescent protein (GFP) and other fluorescent proteins[14]. This led to the creation of GECIs by combining fluorescent proteins with calcium-binding proteins such as troponin or calmodulin[15–18]. GECIs have come to be the tool of choice for most 2PCI applications because they hold two major advantages over chemical indicators: they can be targeted to specific cell types much more efficiently and they can be used for chronic imaging over weeks or months. The first GECIs utilized fluorescence resonance energy transfer (FRET) between two fluorescent proteins linked by a hybrid peptide consisting of the carboxy terminus of calmodulin and the calmodulin-binding peptide of myosin light chain kinase[19]. Hence, FRET-based GECIs shift their excitation or emission spectra upon binding calcium, but require multiple filter sets for 2PCI. A popular FRET-based GECI, TN-XXL[20], uses troponin as the calcium-binding protein (FIG. 2b). Subsequent generations of GECIs have shifted to using a single

fluorescent protein and circularly permuted versions of GFP, together with a calmodulin domain[21,22] (FIG. 2c). These single-fluorophore GECIs exhibit increases in fluorescence emission upon binding calcium when excited at a single wavelength, which simplifies imaging considerably, allowing GECIs to be visualized using standard microscopy filter sets. The Janelia GCaMP family of such GECIs is now on its eighth generation, with variants optimized for speed, brightness and sensitivity for the detection of single action potentials[23]. Other variants exist in a suite of different colours[24–26], or with modifications for subcellular targeting, for instance to the neuronal soma[27,28] or to axons[29]. Dendrite and dendritic spine imaging can be achieved by patching individual

a Chemical (e.g. Indo-1, Fura-2, Fluo-4)
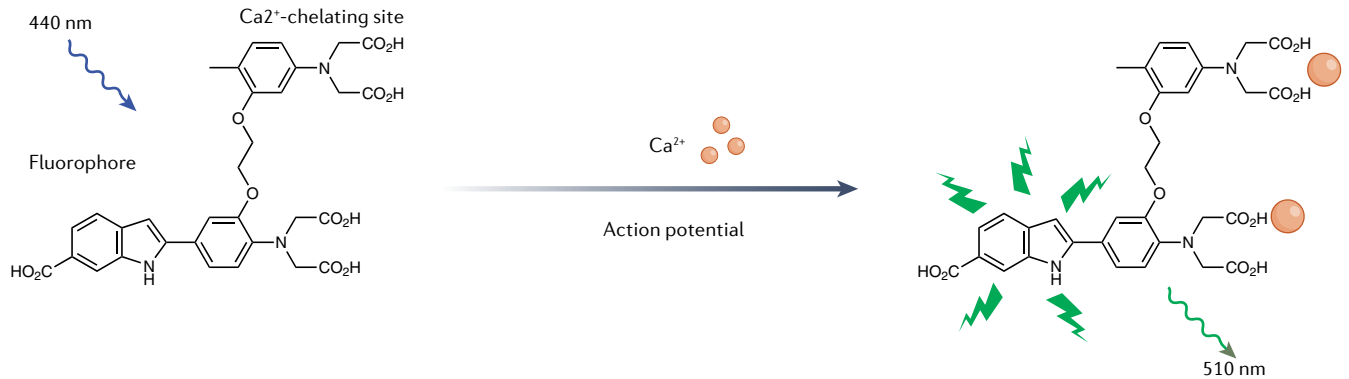
b FRET-based GECI (e.g. TN-XXL)
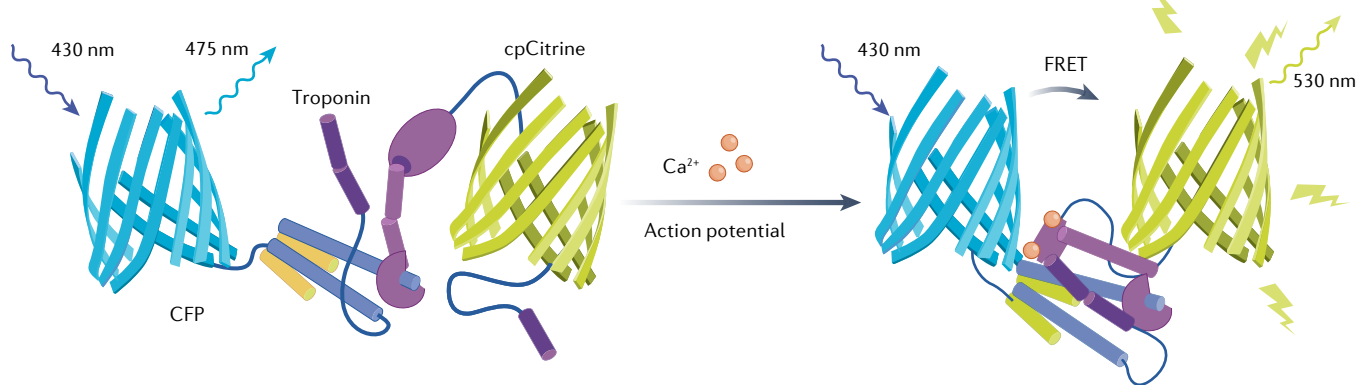
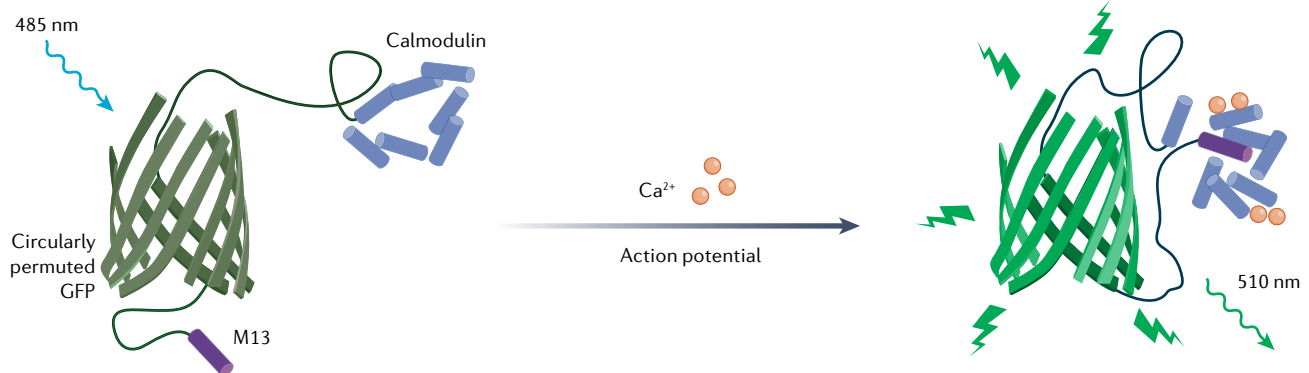**c Circularly permuted GFP-based GECI (e.g. GCaMP6s)**

Fig. 2 | **Types of calcium indicators. a** | Synthetic chemical indicators, which include Indo-1, Fura-2 and Fluo-4, possess a fluorophore domain and a calcium-binding domain (chelating site). When these indicators bind to calcium, their fluorescence intensity increases or decreases. **b** | Fluorescence resonance energy transfer (FRET)-based genetically encoded calcium indicators (GECIs), including TN-XXL, combine a calcium-sensing domain (for example, troponin) with a pair of complementary fluorescent proteins. In the case of TN-XXL, one donor protein (cyan fluorescent protein (CFP)) has an emission spectrum that highly overlaps with the absorption spectrum of the acceptor protein (citrine, or yellow fluorescent protein). A conformation change in the sensing domain induced by calcium brings the fluorescent proteins into close proximity, such that the FRET acceptor will increase its fluorescence by absorbing a fraction of the energy that would otherwise be emitted as photons by the FRET donor. **c** | GECIs based on circularly permuted green fluorescent protein (GFP), including GCaMP6s, are single-wavelength indicators in which circularly permuted GFP is linked to the calcium-sensing protein (typically calmodulin) and the M13 peptide from myosin light chain kinase. Upon calcium binding, calmodulin undergoes a conformational change and tightly binds to M13, preventing water molecules from accessing circularly permuted GFP, which in its anionic form fluoresces brightly.

neurons in vivo and loading chemical calcium indicators, or via transgenic driver lines[30] and/or recombinant adeno-associated viruses (AAVs)[31] that express GECIs sparsely in neuronal subpopulations.

Selecting a calcium indicator. When choosing a calcium indicator, several considerations should come into play[10]. For example, only ratiometric indicators (such as Fura-2) can be used to measure the absolute $[Ca^{2+}]_i$ and are less sensitive to photobleaching. Chemical indicators are excellent for acute preparations, whereas GECIs are ideal for chronic imaging and offer cell type specificity. Red-shifted indicators are ideal for deep imaging, but present versions (such as jRGECO1a and RCaMPs) suffer from less sensitivity than their green counterparts. Indicators with low baseline fluorescence (Fluo-4, several GCaMP variants) can be attractive because of their large dynamic range (higher signal-to-noise ratio), but it may be challenging to identify neurons with low levels of activity.

Introducing calcium sensors

Chemical indicators are usually injected directly into the tissue using a glass micropipette. For GECIs their expression requires delivery of genetic material encoding the sensor into cells. This is most commonly accomplished by injection of a recombinant AAV encoding the desired GECI directly into the brain area of interest[32] (FIG. 3a). This can be done in adult mice, and even shortly after birth at postnatal day 1 (REF.[33]). Importantly, AAVs exist with a range of serotypes[34], which differ in their ability to infect various cell types. It is also possible to package into the AAV backbone different promoters, enhancers[35,36] and other modifications, such as Cre-recombinase or Flp-recombinase dependency, to allow for precise cell type-specific targeting[37] either alone or in conjunction with transgenic reporter mouse lines[38]. Newer AAV serotypes, such as AAV-PHP.eB, can now achieve widespread expression of GECIs in the central nervous system after systemic (intravenous) injections[39]. However, the transduction benefits of systemically administered AAV-PHP.eB appear to be dependent on the mouse strain[40]. One can also take advantage of retrograde viruses or anterograde trafficked trans-synaptic viruses to express GECIs in subsets of neuronal populations that project to or receive projections from specific brain regions, as well as anterograde viruses to record from only axon boutons (FIG. 3b).

Although generally devoid of serious side effects, AAV-mediated expression of GECIs can lead to nuclear filling by the GECI[41,42] presumably because of high expression, either due to delivery of a high concentration of virus or from prolonged expression. These filled cells can show either no activity or aberrant neuronal activity, but as long as they are rare, they do not appear to affect circuit function more widely[41,42]. Alternatively, several transgenic mouse lines have been developed to enable stable, chronic expression of GECIs either constitutively under the *Thy1* promoter[43] or in a Cre-dependent, cell type-specific manner[38,44] (FIG. 3c). Expression is more stable than with recombinant AAV, and nuclear fillin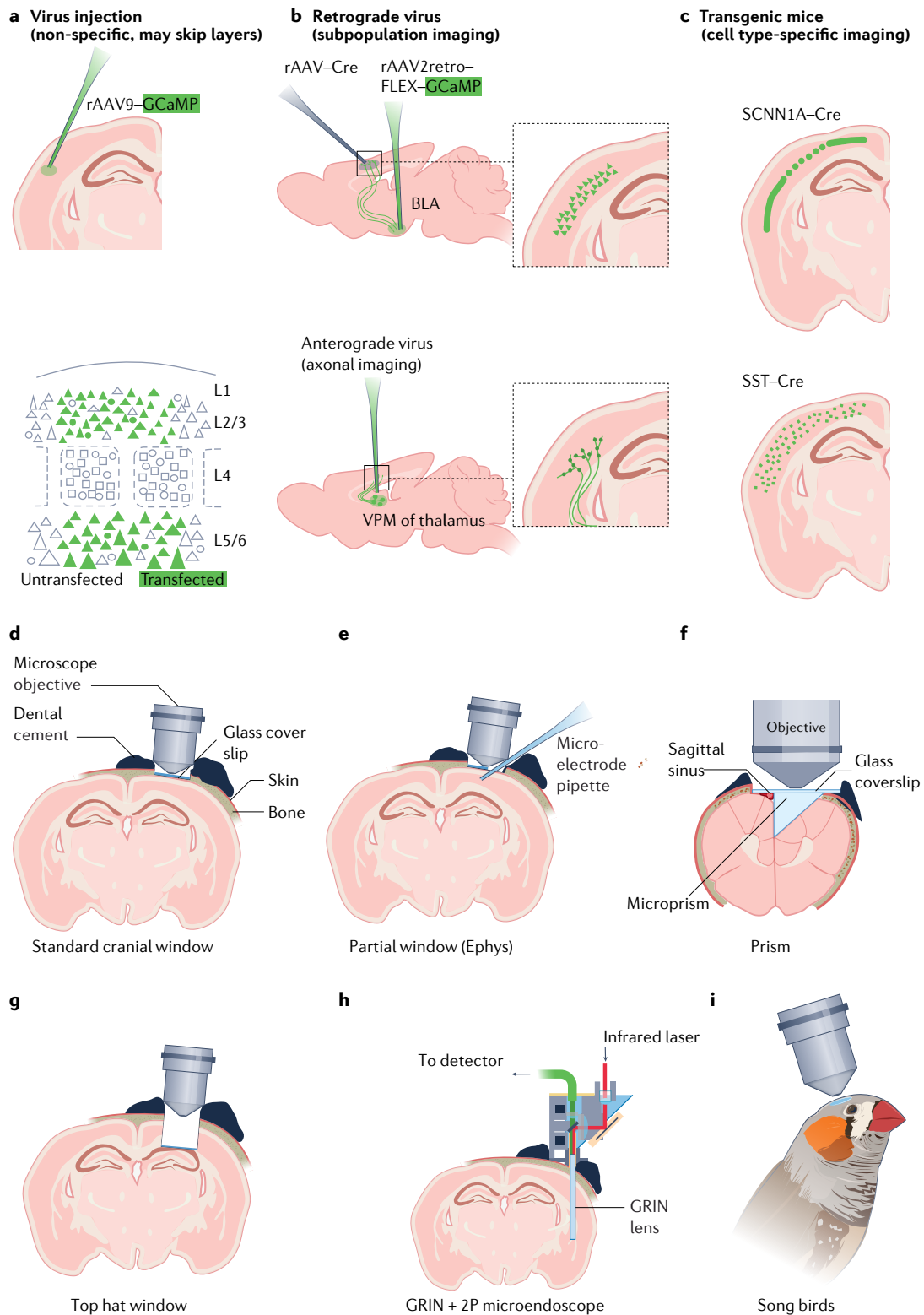g is not typically observed, making transgenic expression of GECIs more attractive for chronic imaging experiments. However, spontaneous epileptiform activity has been detected in several Cre-dependent GCaMP6 lines when crossed with certain Cre-driver lines[38,45]. This may be due to broad central nervous system expression of the tTA2 transcriptional activator early in development and can largely be avoided with careful selection of Cre-driver lines[38].

Optical access to the brain

The next step in a 2PCI experiment is to gain optical access to the brain of animals with skulls. Two main approaches include the open skull window[46] (FIG. 3d) and the thinned-skull preparation[47]. The thin skull approach is less invasive, with minimal activation of microglia and astrocytes in the underlying cortex[48], but the procedure can only be repeated once, limiting its utility for chronic 2PCI[49]. By contrast, because the open skull window provides permanent access to a larger portion of the cortex and affords better resolution of deeper structures, it is more commonly used for 2PCI experiments. Several protocols are available for training in cranial window implantation, including a video demonstration[50]. Robotic devices have been developed to automate cranial window surgery[51,52]; however, these technologies have not been thoroughly tested or widely adopted, presumably owing to their cost and/or their variable success.

With open skull windows, imaging can occur acutely, immediately after surgery or chronically, over many weeks or months. Window quality generally improves 1–3 weeks after surgery, coinciding with the resolution of transient increases in microglia and astrocytes in the tissue underlying the window[46]. It is also possible to implant larger glass-covered windows to enable cortex-wide imaging[51,53].

Modifications of the open skull window have been developed for specialized 2PCI applications, such as partial windows for simultaneous electrophysiology (FIG. 3e) or the use of silicone-based polymer films[54] instead of glass, which allows for the insertion of microelectrodes or micropipettes to deliver drugs. Microprisms can also be implanted in the fissures between hemispheres to image medial brain structures such as the prefrontal cortex[55] or across multiple cortical layers simultaneously[56,57] (FIG. 3f). Other approaches aim to reach neurons in deeper brain regions by aspirating the cortex and implanting glass cannula plugs (sometimes referred to as the top hat window; FIG. 3g) for imaging the hippocampus[58–60] or the striatum[61], or by inserting gradient refractive index (GRIN) lenses[62–64] (FIG. 3h). 2PCI with GRIN lenses has been used to record from deep regions such as the hypothalamus[65], the prefrontal cortex[66], the orbitofrontal cortex[67] or the ventral posteromedial nucleus of the thalamus[68]. These lenses project the 2P scanning pattern into the focal plane of the objective for imaging of deep structures[6] and can be combined with miniaturized 2P microscopes for in vivo imaging in freely moving mice[69,70] (FIG. 3h). Finally, attempts have been made at using optical clearing agents to enable 2P imaging through the intact skull[71], but, to date, these have limited efficacy in adult animals and enable only very superficial imaging.

a Virus injection
(non-specific, may skip layers)

rAAV9–GCaMP

L1
L2/3
L4
L5/6

Untransfected Transfected

b Retrograde virus
(subpopulation imaging)

rAAV–Cre rAAV2retro–
FLEX–GCaMP

BLA

Anterograde virus
(axonal imaging)

VPM of thalamus

c Transgenic mice
(cell type-specific imaging)

SCNN1A–Cre

SST–Cre

d

Microscope
objective
Dental
cement
Glass cover
slip
Skin
Bone

Standard cranial window

e

Micro-
electrode
pipette

Partial window (Ephys)

f

Objective
Sagittal
sinus
Glass
coverslip
Microprism

Prism

g

Top hat window

h

To detector
Infrared laser
GRIN
lens

GRIN + 2P microendoscope

i

Song birds

2P microscopy for calcium imaging

The development of 2P microscopy[72], which allows
high-resolution and high-sensitivity fluorescence detec-
tion in highly scattering brain tissue in vivo, was one of
the most important breakthroughs in neuroscience[73]. In
2P microscopy, two low-energy near-infrared or infra-
red photons cooperate to produce a transition from the
ground to the excited state in a fluorescent molecule. This
2P effect must occur within a femtosecond time window,
which requires ultra-fast lasers that provide short pulses
(80–120 fs) containing a high photon density. All emitted
photons that are transmitted to the photodetector at any
given time, whether ballistic or scattered, can be used to
generate the image[74]. The typical excitation wavelengths

◀ Fig. 3 | **Expressing GECIs in the brain and common window preparations for in vivo imaging. a** | Virus injection directly into the brain. Depending on the virus strain, some cell types may not be transfected (for example, layer 4 with adeno-associated virus 1 (AAV1), AAV5 or AAV9). Triangles and circles represent excitatory and inhibitory neurons, respectively, and squares represent layer 4 spiny stellate neurons. Not shown are systemic virus injections. **b** | Virus injection strategies: retrograde virus injection strategy for labelling somata of subpopulations of neurons that project to a particular brain region and standard anterograde virus injection strategy for labelling axons. Not shown are trans-synaptic anterograde viruses, or viruses that are injected systemically, such as in the tail vein. **c** | Transgenic mice can be used for two-photon calcium imaging (2PCI) of specific cortical layers (SCNN1A–Cre), cell classes (SST–Cre) or subcortical brain regions (not shown). SCNN1A–Cre line and SST–Cre line restrict expression to layer 4 cortical neurons and somatostatin inhibitory interneurons, respectively. **d** | Standard cranial window for imaging neocortex. The skull is removed but the dura and underlying cortex are left intact. **e** | Partial window for simultaneous electrophysiology. **f** | Prism for imaging medial structures or across all cortical layers. A prism is inserted into a fissure or through a cut into the cortex. **g** | Top hat window for imaging hippocampus or striatum. The skull is removed, the cortex aspirated and a glass plug inserted into the brain to gain optical access to deeper brain structures. **h** | Micro-endoscope with gradient refractive index (GRIN) lens for imaging deep structures or for imaging in freely moving mice with a miniaturized, portable two-photon (2P) microscope. Note that GRIN lenses can be used alone, as an optical relay for a standard 2P microscope, which is ideal for 2PCI in subcortical brain structures in head-fixed mice. **i** | Cranial windows for in vivo 2PCI can also be implanted in other vertebrate species besides mice/rats, including zebra finches (shown) or non-human primates. BLA, basolateral amygdala; GECI, genetically encoded calcium indicator; VPM, ventral posteromedial nucleus.

PMT gain
The photomultiplier tube (PMT) output charge per detected photon, which can be adjusted by adjusting the voltage applied to the PMT.

in the near-infrared or infrared spectrum penetrate tissue more readily than does visible light used in conventional one-photon microscopy[75]. Consequently, 2P microscopy can routinely resolve tiny cellular structures, such as dendritic spines, even hundreds of micrometres deep in the brain[46,76]. Consequently, 2PCI has become the method of choice for in vivo recordings in neural circuits of living animals, where the neural connections remain intact.

The basic optical layout of a 2P microscope (FIG. 4) involves a pulsed laser as the source of excitation light, a power modulation system (for example, Pockels cell or half-wave plate), a mechanical shutter, a beam scanning system, an objective and a photodetector (usually one or more photomultiplier tube (PMT)) to detect the generated fluorescence. The typical scan system is composed of lightweight galvanometer-mounted mirrors (galvos for short). A pair of galvos that rotate along orthogonal axes direct the beam in the x–y plane (perpendicular to the optical axis), either in a 2D raster scanning pattern (FIG. 4c) or along a single 1D line scan. Standard 2P lasers used in 2PCI are tunable from 700 nm to 1,040 nm, which is suitable for the excitation of most calcium indicators. More recent lasers that can be tuned further into the infrared spectrum (>1,080 nm) enable the efficient excitation of red-shifted fluorophores for improved tissue penetration[77,78]. Cost-effective alternatives to tunable lasers include single-wavelength fibre lasers — a very recent development being the 1,040 nm lasers — ideally suited for imaging red GECIs[79]. Some microscope systems combine standard galvos (for the y axis) with resonant mirrors (for the x axis), which scan the tissue at a fixed speed (8 or 12 kHz resonance frequency). The ideal objectives for 2PCI have a moderate magnification (16–25×), a high numerical aperture (>0.8) and a long working distance (>2.0 mm), which makes it possible to pass a patch-clamp electrode for simultaneous

electrophysiology. Multi-alkali PMTs are sufficient, but gallium arsenide PMTs (GAsP) are preferred for 2PCI because of their greater sensitivity.

Producing the image
In 2PCI, the image of the tissue is obtained by sweeping the laser across the sample in raster scanning mode (FIG. 4c) with galvo/galvo or galvo/resonant mirror combinations. Even though commonly used fluorescent calcium indicators function as low-pass filters of action potentials occurring on the timescale of milliseconds, sub-second time resolution is still required in calcium imaging. Still, the ideal goal is to sample neurons as fast as possible. In that sense, raster scanning is wasteful because so much of the sampling is devoted to structures that are not of interest to the experimenter, such as blood vessels and the neuropil. Hence, some systems use the same mirrors or acousto-optical deflectors (AODs) to achieve targeted path scanning[80] or random-access scanning[81,82] (FIG. 4c). These create more efficient scan paths, thus maximizing the time spent over structures of interest. Efficient scanning that includes more neurons at the same speed can also be accomplished with spatio-temporal multiplexing[83,84] and piezoelectric devices to move the objective[85] (FIG. 4d).

Unidirectional and bidirectional raster scanning have advantages over targeted path scanning or random-access scanning. First, the 2D images produced can be registered post hoc to correct for movement, which is often necessary when collecting data from awake, behaving animals. Second, raster scanning with a resonant–galvo system can provide frame rates that are sufficient to reveal neuronal activity dynamics on the timescale of behaviour (512 × 512 pixels at 30–40 Hz, or higher if the number of pixels is reduced)[86,87]. Third, raster scanning provides several samples per neuron that can be averaged together to increase the signal-to-noise ratio. Nowadays, most microscopes for 2PCI use resonant–galvo mirror combinations[88–90]. Ultimately, when it comes to signal-to-noise ratio for current GECIs (such as GCaMP6), little is gained by sampling faster than ~30 Hz, given their limited sensitivity and the slow kinetics of their rise time.

In generating high-quality 2PCI images it is also important to consider the trade-offs between scanning speed and signal. At greater speeds, the pixel dwell time is reduced, which leads to fewer 2P excitation events and fewer photons emitted by the calcium indicator. Whether using custom-built or commercial 2P microscopes, the acquisition software allows for the independent control of the laser power and the PMT gain. These parameters must be carefully adjusted to improve the signal-to-noise ratio (BOX 1). In general, all acquisition parameters will depend on experimental conditions — such as the type of GECI and levels of expression, depth of imaging, species, quality of window and so on — and should therefore be optimized for each experiment[91].

Safety and ethical considerations
Importantly, 2PCI requires the use of powerful Class IV lasers that generate peak power of several megawatts. These lasers are dangerous and can cause burns to

exposed skin and severe eye injury causing permanent blindness. Investigators embarking on 2PCI experiments should consult with the laser safety committees at their research institutions and seek training and approval for the use of these lasers in their laboratories. 2PCI in vertebrate animals requires survival surgeries that are invasive — involving implantation of cranial windows or GRIN lenses and intracerebral virus injections.

Thus, it is critical to consult with veterinarians and seek adequate training in these procedures prior to starting these studies.

Results

In this section, we describe the expected imaging results from a 2PCI experiment, how to process those images and methods for analysing the subsequent data.
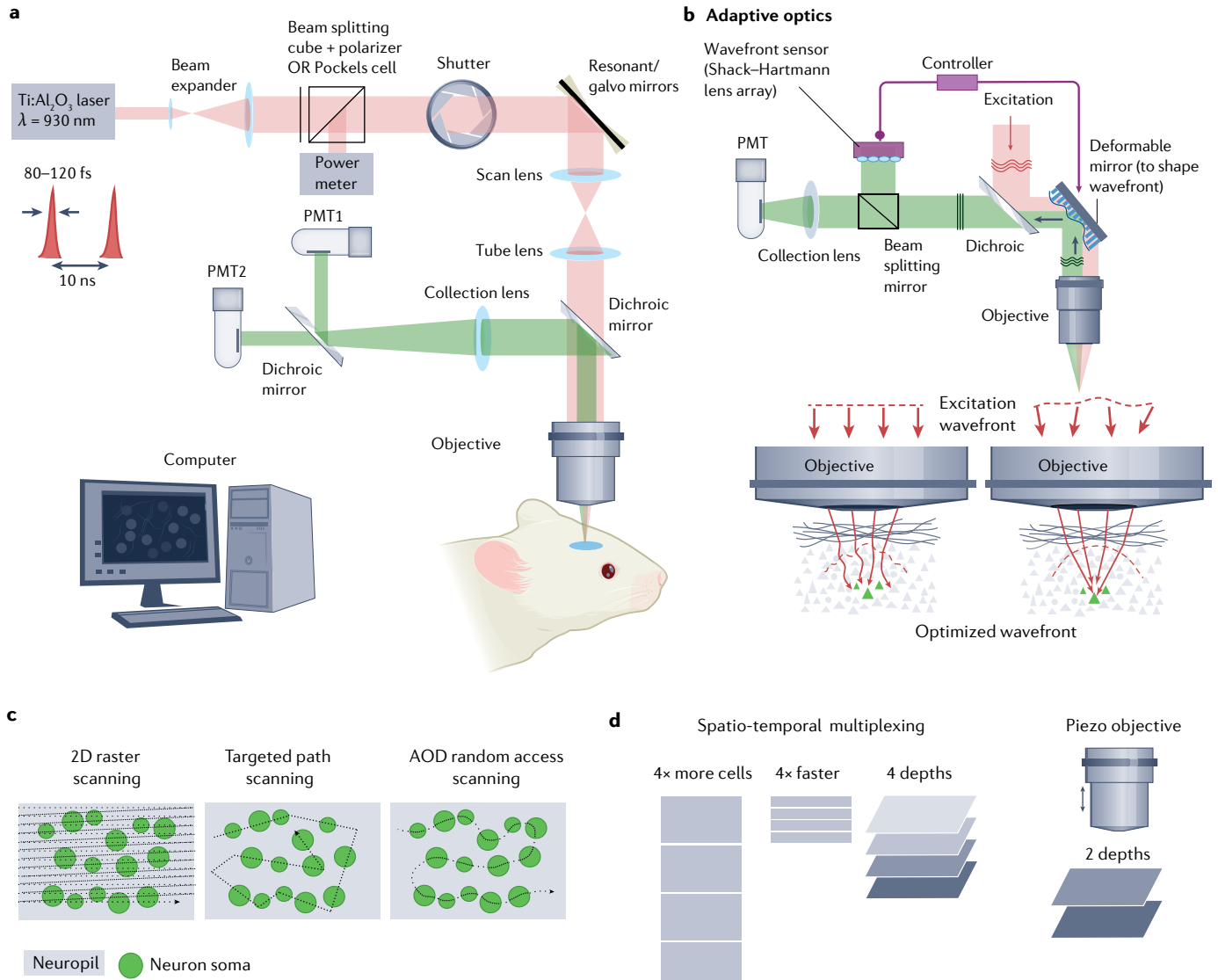

Fig. 4 | **Components of a 2P microscope, adaptive optics and scanning approaches for high-speed and volumetric 2PCI. a** | Two-photon (2P) microscope and its components, including the Ti:sapphire laser, a beam expander (used to ensure slight overfilling of the back aperture of the objective lens), a half-wave plate combined with a polarizing cube or a Pockels cell to control and measure the laser power, a shutter to control exposure, scanning mirrors, a scan lens, a tube lens, a dichroic mirror, the objective lens (with high numerical aperture and long working distance), a collection lens, the photomultiplier tubes (PMTs) and a CPU to integrate and control the image acquisition process. **b** | Adaptive optics for wavefront optimization and improved depth penetration. Top: modified emission path in 2P microscope that includes a wavefront sensor (Shack–Hartmann lens array) to estimate the degree of aberrations, and a deformable mirror to shape the excitation beam to compensate for those aberrations. Bottom: uncompensated wavefront distorted by sample inhomogeneities (left) and optimized wavefront after adaptive optics (right). **c** | Various scanning patterns in two-photon calcium imaging (2PCI). Dotted lines indicate scanning path. Spacing of dots indicates relative speed of scanning. **d** | Techniques for imaging volumes. In spatio-temporal multiplexing (left), the excitation beam is split into n beamlets that are slightly delayed in time with respect to one another, which can be used to image n times faster, or in n planes. Fluorescence resulting from each beamlet can be separated in time by the PMT, provided that $n \times$ fluorescence decay time of the genetically encoded calcium indicator (GECI) does not exceed the repetition rate of the laser (80 MHz). For piezo-moving objectives (right), two or more planes at different depths can be scanned in quick succession with the use of a piezo motor that moves the objective quickly to each of those depths. AOD, acousto-optical deflector; galvo, galvanometer-mounted mirror.

Optical access

Obtaining high-quality, reliable results from 2PCI experiments starts with clear optical access to the sample. For the thinned-skull method[47], the consistency and ultimate thickness of the skull are essential. Insufficient thinning will preclude high-resolution imaging of smaller or deeper structures, and non-uniformity will introduce spherical aberrations that distort the images. Excessive thinning can lead to brain inflammation, dendritic blebbing or scarring of the dura that prevents multiple longitudinal imaging sessions. When using a transparent optical element (such as glass windows or a GRIN lens), there are different reasons — both acute and delayed — for compromised 2PCI data (FIG. 5). Acutely, the dura covering the brain may be bruised or punctured during the drilling, causing a brain haemorrhage (FIG. 5b). The blood is usually reabsorbed over the following days or weeks, which may reassure experimenters and prompt them to keep the animal in the study. However, even the slightest bleeding can negatively affect the underlying brain tissue (because of direct injury, scarring or inflammation), which is likely to impact neuronal activity. Experimental animals in which the cranial window surgery led to puncturing the dura or bruising of the brain should be rejected. With glass plug or GRIN lens approaches, the dura and brain tissue are damaged or removed, which could potentially disrupt aspects of the connectivity that is being investigated. Naturally, preparations spoiled by air bubbles, excess cyanoacrylate glue, dental cement or other foreign bodies (such as hair) under the glass should also be rejected. Delayed problems with cranial windows that universally complicate imaging include the gradual appearance of bone growth (FIG. 5c) or granulation inflammatory tissue under the window, which render the window opaque. Some groups have resorted to stacking glass coverslips for traditional cranial windows to prevent bone regrowth[92], but the utility of this approach has not been carefully assessed. The brain tissue under the window may occasionally appear sunken, which could be due to tissue heating from prolonged drilling, infection or non-specific trauma. The dura may also become hypervascularized, which also precludes imaging. All of these defects are usually readily apparent by simple visual inspection of the optical preparation.

Imaging results

High-quality 2PCI also depends on optimizing image acquisition, including ensuring appropriate loading or expression of calcium indicators, optimizing image acquisition parameters and minimizing motion artefacts. For most chemical calcium indicators, individual cells should appear uniformly filled with the indicator, although brightness may vary slightly amongst different cells based on differential dye uptake[12]. Imaging takes place after a period of loading (generally 60–90 min), when cellular uptake of the dye has reached a steady-state level, but before there is significant dye efflux (after 3–4 h), which causes an unstable baseline fluorescence and difficulty calculating change in fluorescence ($\Delta F/F$) values. For GECIs, on the other hand, in an ideal preparation indicator expression should largely be excluded from the nucleus, resulting in a doughnut-shaped appearance at the soma (FIG. 5d). Cells with nuclear filling should be excluded from subsequent analysis; in fact, experimenters should consider excluding entirely data sets with large numbers of filled cells.

Image acquisition parameters (laser intensity, PMT gain and so on) should be set such that baseline fluorescence is visible for cells of interest to enable calculation of $\Delta F/F$ values. On the other hand, there must be sufficient dynamic range that PMTs are not saturated during calcium transients when fluorescence increases, which would result in loss of information on the true amplitude and duration of calcium transients. Baseline fluorescence values should be stable throughout the duration of recording. If baseline fluorescence fluctuates significantly, this could indicate photobleaching due to excessive laser intensity or focus drift. Focus drift can come from physiological sources (animal heartbeat or breathing), licking during behaviour[93] and other animal movements (running and self-grooming), or from mechanical drift of the objective. Within limits, in-plane drift can typically be well compensated for by post-processing motion correction algorithms, whereas out-of-plane movement is more problematic.

In addition to photobleaching, high laser power can also cause direct phototoxicity to imaged structures, particularly when repeatedly scanning over a small area, so reporting the average laser power at the sample is critical. Phototoxicity is a non-linear process and may result from free radical formation and/or heating of tissue. Under typical conditions, in vivo imaging through a cranial window may cause temperature increases of ~1.8 °C per 100 mW of laser power[94]. Although tissue injury with 2P excitation may be apparent after 20 min of continuous illumination at >250 mW, 2PCI experiments typically require much lower power at the sample. On the other hand, photodamage may be a greater concern when combining 2PCI with 2P optogenetic stimulation, as this requires considerably more total laser exposure[95].

Box 1 | Signal-to-noise issues

The quality of two-photon calcium imaging (2PCI) data depends significantly on the signal-to-noise ratio, with higher values being desirable. Sources of noise in 2PCI include photomultiplier tube (PMT) noise when wayward electrons are incorrectly registered as actual photons, which can be avoided by decreasing PMT gain; dark noise and other technical noise types; and shot noise, which owes its existence to the fact that fluorescent photon emission follows a Poisson process. If, on average, a single photon is emitted per pixel of a fluorescing sample within a particular time interval, then the randomness of fluorescence generation makes it impossible to predict what will happen when this pixel is sampled; sometimes one photon will be detected, sometimes none, sometimes two, rarely even more. This difference between the number of photons emitted and the true emission rate is commonly referred to as shot noise.

The achievable signal-to-noise ratio in shot noise-limited imaging, such as 2PCI, is proportional to the square root of the total fluorescent photon flux[1]: the more photons emitted, the higher the signal-to-noise ratio. One can boost this value by increasing the pixel dwell time, by adjusting the concentration, calcium affinity, brightness and photostability of the indicator, and by optimizing the excitation and collection efficiencies of the imaging system. Although increasing the dwell time or the excitation power may produce an initial gain in signal-to-noise ratio, photobleaching and photodamage may be unsustainable.

The signal-to-noise ratio requirement sets the range of photon counts that must be obtained for each neuron at each time step[254] and will depend on the experiment. Some biological questions may require high signal-to-noise ratio measurements, whereas others need more qualitative measurements of changes in activity, where the signal-to-noise ratio can be slightly compromised to image more neurons simultaneously.
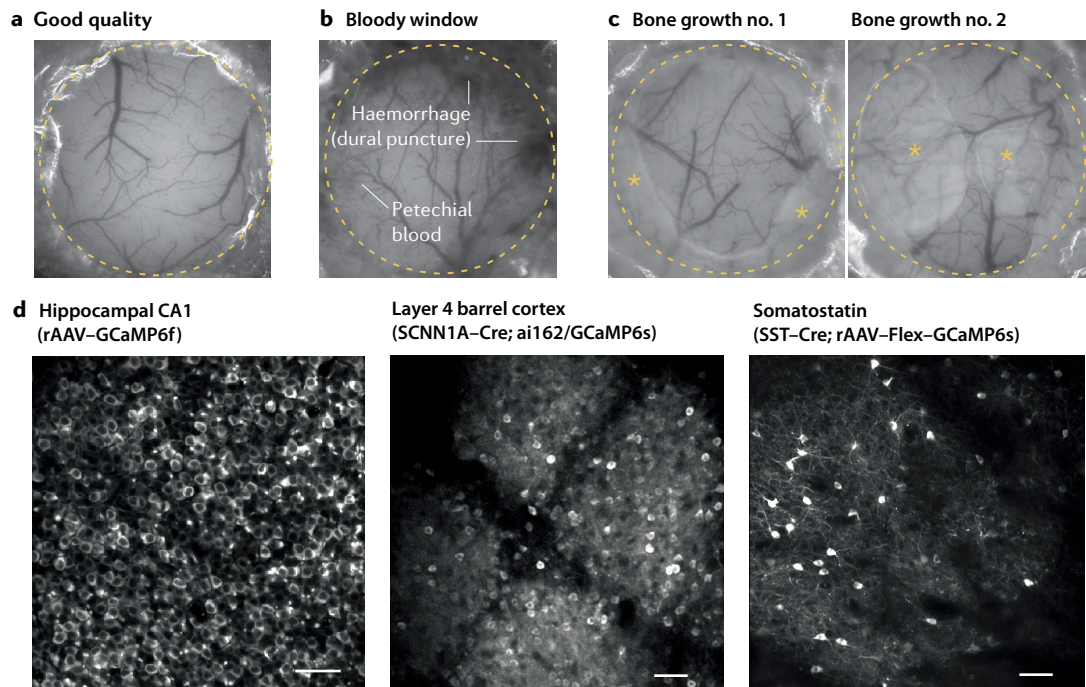

Fig. 5 | **Examples of good and bad cranial windows and fields of view. a** | Example of good-quality cranial window. Blood vessels can be clearly seen and there is no vascular proliferation, blood or bone growth. **b** | Example of a window with frank haemorrhage due to puncture of the dura during drilling or lifting the bone flap. **c** | Examples of windows with bone growth starting at the periphery (left) and excessive bone growth that obscures the middle of the window (right). Asterisks indicate areas of bone growth. **d** | Example fields of view with GCaMP6 expression in hippocampal pyramidal neurons, layer 4 neurons of barrel cortex and somatostatin neurons of barrel cortex. Scale bars are 100 μm. Part **d** images courtesy of N. Kourdougli and A. Suresh.

Data analysis

The final step in 2PCI is the analysis of the data to extract meaningful signals from changes in fluorescence intensity of the indicators and estimate neural activity (FIG. 1c). A minimal set of preprocessing steps (FIG. 6a) are commonly applied to raw multiphoton imaging frames to extract an interpretable correlate of neural activity. These include motion correction, localization of the sources (segmentation into regions of interest (ROIs)) and extraction of relevant signals (calcium traces and deconvolved spike rates). TABLE 1 lists the main algorithms used for these major steps. Several publicly available resources exist in GitHub and other repositories for each of these steps, most of which are customized by their creators for specific data sets. More user-friendly algorithms are also included in the more mainstream packages, such as Suite2p, CaImAn and EZcalcium[96–98] (Supplementary Table 1). In this section, we summarize the typical aspects of these steps, but refer the reader to other works for a more detailed perspective of these analyses[99–101]. We do not discuss downstream analyses of 2PCI data, such as the use of dimensionality reduction and clustering techniques (using, for example, tSNE and PCA) or the use of classifiers/decoders to correlate, for example, neural activity with behavioural measures[102].

Motion correction. Motion artefacts during in vivo 2PCI can cause changes in fluorescence intensity, which not only distort functional signals associated with neural activity but could be falsely interpreted as brain activity[103]. The causes of such motion range from fast shifts or deformations in the field of view due to animal movement (for example, awake mice running on a treadmill or grooming) or scanning defects caused by failing mirrors to slow changes due to brain physiology (such as arteriole pulsations and hydration) and/or imaging set-up imperfections (such as vibrations of the air table). To correct for motion in the x–y plane, frames need to be aligned to a fixed representative reference image by means of a rigid or elastic transformation. The most popular algorithms for such image registration rely on template matching via cross-correlation or phase correlation to estimate shifts between frames and a reference[96,104–106]. These algorithms usually provide integer shifts, but subpixel approximations can be obtained with various approaches. Fast algorithms that provide non-rigid approximations to elastic motion are obtained by parcellating the field of view in multiple overlapping blocks and interpolating the shifts obtained for each block at subpixel resolution[96,104,105]. Other approaches based on more computationally intensive algorithms exist, but their use is not mainstream[105].

Sometimes it is not possible to correct movement of a whole frame/volume and it becomes more convenient to track specific landmarks. For instance, whole brain imaging of freely moving animals with complex deformation patterns (*Caenorhabditis elegans*, hydra or larval zebrafish) requires customized approaches[107]. Similarly, imaging with AODs requires specialized methods[82,108].

Standard motion correction approaches might occasionally fail at correcting rapid shifts, for example owing to motion in the *z* direction. In these rare cases, experimenters may choose to remove the affected frames from the data set, provided they represent a small fraction of the entire data set. To avoid *z*-axis motion artefacts, it is always advisable to stabilize the imaging preparation as much as possible.

Image preprocessing. The goal of this step is to reduce the inherent noise associated with data sets that have a low signal-to-noise ratio or to reduce the size of large data sets, and it can be done before or, most typically, after motion correction. Techniques range from unsupervised linear and non-linear spatio-temporal filtering or down-sampling operations[96,99,109] to supervised approaches[110]. However, drawbacks include the fact
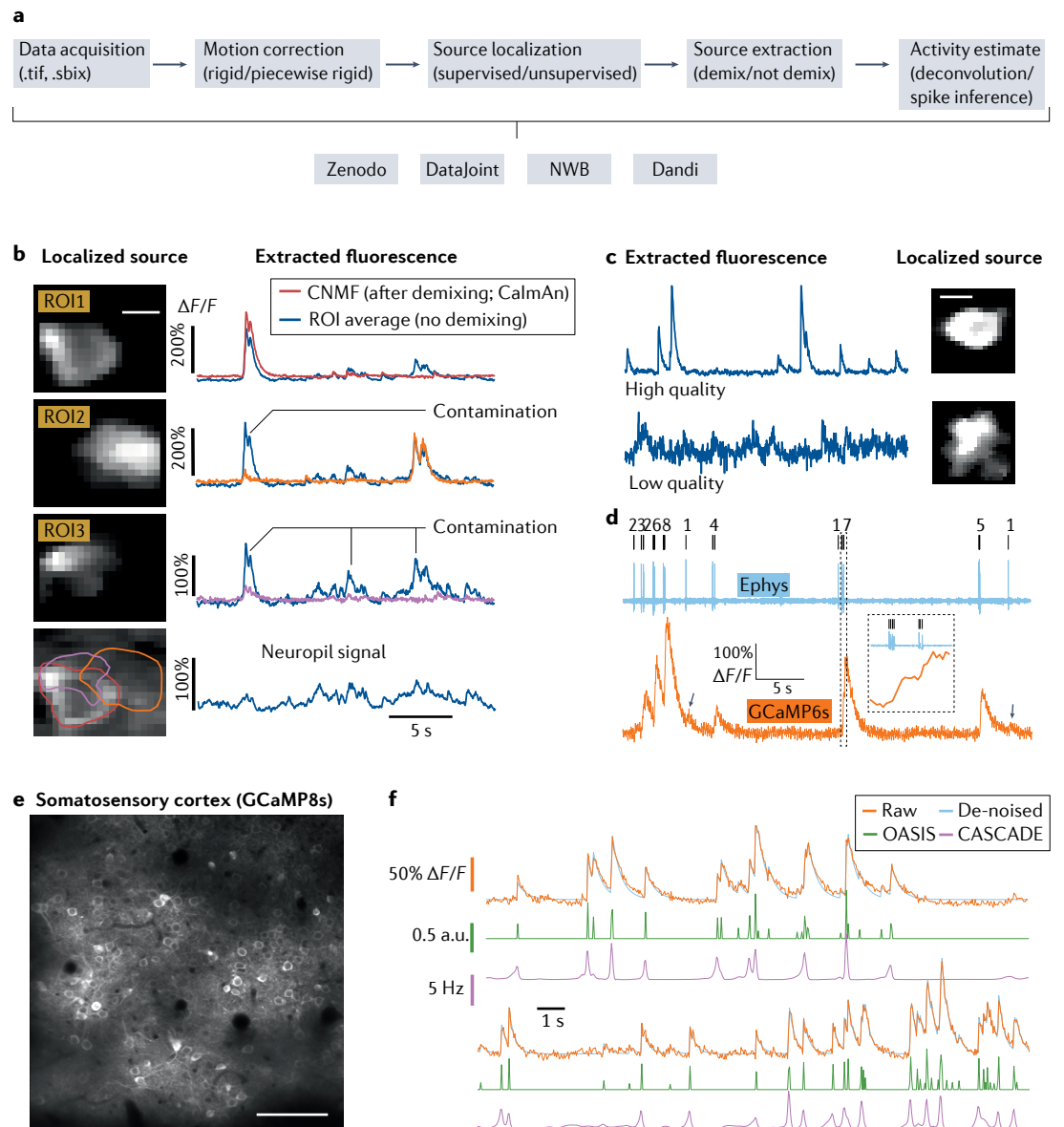

Fig. 6 | **Illustration of analysis pipeline concepts. a** | Analysis pipeline and example relationship to archiving frameworks. **b** | Example of source localization (left) and activity extraction (right). The blue traces represent the raw calcium signal before demixing. The red, orange and purple traces represent the revised traces after demixing to remove contamination from adjacent neurons. Bottom row represents component contours overlaid on the correlation image (left) and the neuropil contamination signal estimated with CNMF (right). Scale bar in ROI1 (10 µm) is the same for all regions of interest (ROIs). **c** | Example of high-quality (top) and low-quality (bottom) temporal (left) and spatial (right) sources extracted with CNMF. Scale bar is 10 µm. Traces in panels **b** and **c** obtained from data used in REF.[84]. **d** | Example of simultaneous GCaMP6s traces from two-photon calcium imaging (2PCI) (orange) and patch-clamp electrophysiology (blue). Number of ground truth spikes shown at top. GCaMP6s is able to detect isolated single spikes (arrows). Traces obtained from data used in REF.[5]. **e** | Field of view of viral expression of GCaMP8s in primary somatosensory cortex of adult mouse. Scale bar is 100 µm. **f** | Example of raw fluorescence signal from GCaMP8s (blue trace) from two cortical neurons and corresponding deconvolved signals. For deconvolution we used CalmAn's OASIS (green trace) or CASCADE (purple trace). ΔF/F, change in fluorescence over the baseline fluorescence; NWB, Neurodata Without Borders.

that filtering/down-sampling operations can reduce the temporal or spatial resolution and, secondly, that linear or non-linear filtering operations might modify the underlying signal properties and render some of the post-processing steps less accurate. To validate de-noising techniques before use, we advise testing the full analysis pipelines on a few example data sets with and without de-noising to identify potential discrepancies in the results.

Localization of the sources. After motion correction, the next step is to localize the source of the fluorescence signals, the individual ROIs. Ideally, this means associating a set of pixels — which are assumed to provide spatio-temporally coherent fluorescence signals — to one or more cellular compartments (FIG. 6b).

This is generally accomplished by applying unsupervised and supervised computer vision algorithms to static images[111,112]. In parallel, temporal correlations can be used to group sets of pixels via unsupervised algorithms[113–116]. It is also possible to manually select ROIs by recognizing the shape of neuronal somata in maximum intensity x–y–t projections, but this is time consuming and can introduce biases, such as missing rarely active neurons owing to dim baseline fluorescence. Inspection of the sources should be conducted after automated source localization in case it is necessary to manually add missed ROIs or remove false sources. In the case of longitudinal in vivo 2PCI across days or weeks, it is desirable to register the ROIs from multiple imaging sessions. Recent algorithms and software packages have been developed to register images and their ROIs across

Table 1 | **Standard algorithms for 2PCI data analysis**

Algorithm	Purpose	When to use	Caveats	Advantages
Motion correction				
Template-based rigid motion correction	Align frames with a rigid translation	Small field of view, fast scanning	Will not capture elastic movements	Computationally efficient, robust
Template-based piecewise rigid motion correction	Align frames with a piecewise rigid approach	Larger field of view, slow scanning	Less robust with low signal-to-noise ratio	Relatively efficient computationally
Landmark-based motion tracking	Align frames with non-linear spatial transformations	Hydra, *Caenorhabditis elegans*	Computationally expensive, less robust with low signal-to-noise ratio	Deals with the most general case
AOD scanning	Track sparsely sampled neurons	Sparse scanning	Difficult implementation	Very high speed
De-noising				
Linear filtering	De-noise frames	Low signal-to-noise ratio	Can reduce spatial and/or temporal resolution and can change signal properties	Easy to implement and use
Non-linear filtering	De-noise frames	Low signal-to-noise ratio	Can reduce spatial and/or temporal resolution and change signal properties	Can be very efficient in removing noise
Source localization				
Summary image source localization	Identify sources from single images	Sparsely labelled samples	Problematic with densely labelled samples	Can detect silent neurons, computationally efficient
Unsupervised spatio-temporal source localization	Identify sources from multiple frames	Dendrites, axons	May be computationally expensive	Does not require training nor shape information
Supervised spatio-temporal source localization	Identify sources from multiple frames	Training data available (somas)	Needs training, needs annotated data, generalization	Computationally efficient
Source extraction				
ROI average	Extract traces from known sources	Sparse expression	Contamination, lower signal-to-noise ratio	Computationally efficient
Matrix factorization	Simultaneously extract sources and traces	Dense expression, high probability of contamination	Computationally expensive, requires initialization	Higher signal-to-noise ratio, more reliable signal
Activity estimation				
Spike deconvolution	Extract a sparse signal from calcium traces	Increase temporal resolution, large data sets	Not directly interpretable	Computationally very efficient
Unsupervised single spike/rate extraction	Approximate spikes/rates	Increase temporal resolution and interpretability	Computationally expensive	Might increase interpretability
Supervised single spike/rate extraction	Approximate spikes/rates	Increase temporal resolution, interpretability	Requires training	Might increase interpretability

2PCI, two-photon calcium imaging; AOD, acousto-optical deflector; ROI, region of interest.

sessions either automatically[97,117] or via semi-manual approaches[96]. Even when care is taken to maintain a stable field of view, some neurons may seem to appear or disappear across imaging sessions, and this should be considered during downstream analysis.

Fluorescence signal extraction. The simplest method to extract fluorescence signals consists of averaging the fluorescence for all pixels belonging to a given source/ROI (FIG. 6b). This method is efficient and straightforward, but the signal can be contaminated from multiple sources, including the neuropil and adjacent neurons above or below the imaging plane, especially when ROI segmentation is done manually[84]. Straightforward approaches exist to subtract the background neuropil signal[113], or to model its signal jointly with neural activity[84]. Many algorithms have been developed for estimating the optimal spatial footprint of sources and their corresponding temporal activity simultaneously, which is particularly important in densely labelled samples. These include non-negative matrix factorization, independent component analysis or dictionary learning. Often, these algorithms[84,96,118] can be initialized with the source localization algorithms described above, or with more recent stand-alone software pipelines dedicated to 2PCI analysis[97,98]. Importantly, non-negative matrix factorization approaches are very effective in separating signals from overlapping neurons and the neuropil as they tend to model its effect on the combined signal[84] (FIG. 6b). Most existing algorithms will require manual curation to remove low-quality components or add missed sources (FIG. 6c).

Next, the extracted fluorescence traces must be normalized to account for ROIs of different baseline fluorescence intensities and to compare activity between and across sessions. The favoured approaches are *z*-scoring the fluorescence calcium traces (with respect to a statistically estimated baseline) or simply computing the change in fluorescence intensity over the baseline fluorescence ($\Delta F/F$)[97,119]. However, these are imperfect approaches that can sometimes lead to incorrect approximations[120]. Expected $\Delta F/F$ values during calcium transients will vary significantly based on the calcium indicator, imaging preparation, cell type of interest and the magnitude of the activity of the cell, but should be clearly visible above the background noise of the signal. For example, we typically exclude from further analysis cells that do not show any calcium transients exceeding three standard deviations above their mean background fluorescence intensity. In layer 2/3 pyramidal cells in the visual cortex, the latest-generation GECI, jGCaMP8s, achieves $\Delta F/F$ values of ~60% for single action potentials on average, and peak $\Delta F/F$ values evoked by drifting sinusoidal gratings ranging from 30% to 1,000%[23].

Spike inference. Calcium traces reflect the firing of neurons, so it should be possible to estimate spike rates from raw fluorescence signals. However, public benchmarks[121] and studies comparing 2PCI with electrophysiology[5] have shown that spike inference is imprecise, mainly because of the low sensitivity and non-linearity associated with calcium indicators. Spike inference is especially challenging for tonically active neurons and those with high firing rates, such as inhibitory interneurons (Supplementary Table 1). Some algorithms for spike inference use deconvolution to estimate a sparse signal that is not directly interpretable as spiking activity[122], whereas others use Bayesian and deep learning methods to infer single spikes or spike rates[123,124] (FIG. 6e,f). Even the latest deep learning tools for spike estimation, trained on extensive 2PCI data sets, provide at best ~0.8 correlation to ground truth electrophysiology[124]. Because different algorithms are more effective for particular data sets, users are advised to try different methods for spike inference and, ideally, to use ground truth experiments with physiology to validate the algorithms (FIG. 6d).

Popular software packages. There are an increasing number of readily available software packages that implement all or part of the outlined analysis pipelines (Supplementary Table 2). Unfortunately, few of these resources are truly plug and play, and even fewer are maintained, updated and improved by the developers.

Applications

In this section, we discuss several recent applications of 2PCI in neuroscience and provide a few representative examples for each. Although we focus on studies of neurons in mice, we also briefly allude to a few other applications of 2PCI in non-neuronal cells and in other species. The goal is to provide the reader with a taste of the range of experiments that can be pursued with this technique, rather than to provide a comprehensive review of the hundreds of published studies.

Typical neuronal physiology

2PCI has been invaluable in probing network activity to understand the vast array of brain functions, from how neuronal populations process and interpret sensory signals or elicit motor actions to how they store memories or trigger emotional responses. Below we provide only a few examples of the kinds of questions that have been uniquely addressed with 2PCI.

Sensory processing. How neural ensembles process sensory inputs to guide decisions, one of the quintessential questions in neuroscience, has been investigated with 2PCI with great success. In the context of how the primary somatosensory cortex (S1) processes whisker inputs in mice, 2PCI has been used to characterize how S1 neurons encode touch and whisker movement[125,126], how their responses mature during development[127], their plasticity after whisker plucking[128] or how they adapt to repetitive whisker stimulation[129,130]. 2PCI has also been invaluable in understanding how local information in S1 is transmitted to downstream cortical regions along segregated processing streams during perceptual discrimination tasks[131].

Connecting neuronal ensemble dynamics to behaviour. There is broad interest in linking neural activity with defined behaviours in awake animals[132]. 2PCI can fulfil this goal in freely moving mice through the use of head-mounted portable 2P microscopes[133–135] or in head-fixed animals using standard 2P microscopes.

The latter strategy is by far the most prevalent approach. For example, a pioneering study examined the function of mouse hippocampal neuronal ensembles in CA1 during a complex virtual spatial navigation task[136]. Numerous studies have adapted this approach to examine neural circuit dynamics in various cortical and hippocampal brain regions[60,137,138]. 2PCI has also been used to study visual sensory processing in awake behaving animals. For example, imaging the visual cortex as mice learn a visual discrimination task can be used to reveal the mechanistic underpinning of improved discriminability of behaviourally relevant sensory stimuli[139–141]. The significant advantage of such experiments involving GECIs is that imaging can be repeated during consecutive days and weeks, again and again, allowing a thorough investigation of the mechanisms of neuronal plasticity associated with learning and memory formation in vivo[142].

Recording from different cell types or cells projecting to specific brain regions. 2PCI can also be used to record from different neuronal cell types, or cells projecting to a particular brain region, taking advantage of Cre/Flp driver lines combined with viral tools for retrograde or anterograde trans-synaptic expression[143]. In the primary visual cortex, recent studies are beginning to elucidate how different subclasses of inhibitory interneurons respond to visual stimuli[140,144,145]. With 2PCI one can visualize spatial relationships of neurons in vivo, so it is relatively easy to track the same cells over periods of days or weeks with high confidence, something that is much more challenging with silicon probes (although potentially feasible with the latest-generation Neuropixels 2.0 probes[146]).

Circuits across species. In some species, electrophysiology is either not feasible or extremely challenging because of the small size of the animal (*C. elegans*) or because its exoskeleton keeps contents under pressure (*Drosophila*), so 2PCI is the preferred alternative. Some animals such as zebrafish embryos or *Drosophila* larvae seem ideally suited for 2PCI because their small size and transparency make it possible to record from thousands of neurons simultaneously[147]. Although the use of chemical calcium dyes[4] enables 2PCI in virtually any species, targeted expression of GECIs is much easier in genetically tractable model organisms. As a result, mice, worms, flies and zebrafish have usually benefited from testing novel classes of indicators at early stages of development[23,41,42]. By contrast, expressing such indicators in other species that are less widely supported often requires extensive exploration in terms of AAV serotypes, promoters, GECIs and so on. In some cases, compelling interest in the field has led to the generation of transgenic non-human primates, such as marmosets, that express GECIs[148]. 2PCI has now been used in many different species, from zebra finch songbirds[149] to macaque monkeys[150,151].

Calcium imaging in vitro. Acute slices and organotypic slice cultures of brain tissue offer several advantages over in vivo studies in live animals. Beyond their lower cost and smaller footprint, slices lend themselves more easily

to precise optogenetic manipulations as they are not influenced by external inputs or brainstem neuromodulation (brain states). Traditionally, slices have been ideal for conducting patch-clamp recordings of single neurons to investigate synaptic currents, intrinsic properties or simultaneous recordings from a handful of neighbouring neurons to study local connectivity. Slice electrophysiology has also been combined with optogenetics for channelrhodopsin-assisted circuit mapping of local and long-range projections to single neurons[152]. However, with calcium imaging it became possible to record from hundreds or thousands of neurons simultaneously across cortical layers, or in deep brain regions that would be inaccessible to in vivo calcium imaging. Elegant in vitro 2PCI studies were the first to reveal attractor dynamics and synfire chains in neocortical circuits[153,154] or how circuits can learn time intervals[155]. More recently, 2PCI of activity within cerebral organoids has made it possible to record spontaneous activity from developing neurons derived from human IPSCs[156]. We are likely to learn a lot from 2PCI of organoids in the coming years.

Emergent properties of circuits and sensory percepts. Neuronal ensembles or assemblies (which refer to when subsets of neurons reliably fire together) constitute the flexible building blocks of sensory perceptions, motor programmes or memories[157–159]. Indeed, the activity of such ensembles encodes information that is not (or cannot be) reliably encoded by single neurons[160]. These emergent properties of neuronal circuits are reliably observed with techniques such as 2PCI that allow the simultaneous measurement of the activity of large numbers of spatially distributed neurons. It is now possible to combine two-photon holographic stimulation of specific neuronal ensembles with 2PCI[161,162] to trigger behaviours, something that would not be possible with electrophysiology. In a landmark study, optogenetic activation of only a subset of neurons within a given ensemble that was activated during a visually guided go/no-go task was able to generate the appropriate behavioural response if it could reliably trigger the replay of the entire ensemble activity[163]. 2PCI has even been used in optical brain–computer interface experiments based on calcium signals of cortical neuronal ensembles[151,164].

Subcellular compartments. Although 2PCI is most often used to record activity at the soma, it can also be used to record from dendrites and axons. Patch-clamp electrophysiology can target some of the larger dendritic branches in vitro and in vivo, but it cannot be used to record from single dendritic spines. Using in vivo 2PCI, it is not only possible to record back-propagating action potentials in dendrites but also spontaneous calcium transients occurring in single dendritic branches or even spines to discover the previously unanticipated roles they play in learning and memory[165,166]. Algorithms exist for distinguishing back-propagating action potentials from local calcium transients in dendritic segments or individual spines[167]. 2PCI of axonal boutons can also be a useful strategy to record activity from neurons located deep in the brain or in distant cortical regions that project to the particular cortical area under investigation[168,169].

Disease and other conditions

After decades of gaining insight into the basis of neurologic and psychiatric disorders from anatomical studies, neuroscience is increasingly turning its attention to disruptions in brain activity. Recording network activity may be particularly relevant in animal models of certain neuropsychiatric disorders, such as autism, depression, epilepsy or schizophrenia, for which neuroanatomical clues may be lacking. In this context, the impact of calcium imaging has been remarkable. Providing cellular resolution where EEG (or functional MRI) could not, 2PCI has documented changes in the activity of single neurons, or populations of neurons, during development, adulthood and ageing, in mouse models of neurodevelopmental conditions (such as autism and schizophrenia), Alzheimer disease, epilepsy, stroke and so on. Below we highlight only a few examples of how 2PCI has revealed novel circuit mechanisms in autism, Alzheimer disease and stroke, as examples of neurodevelopmental, neurodegenerative and acute injury entities, respectively.

Autism. In the context of autism, changes in network synchrony during early development were first reported with 2PCI in the past decade[170–172]. More recently, 2PCI studies with GECIs have revealed more subtle differences in sensory evoked activity in the neocortex, including reduced activity of parvalbumin interneurons in multiple mouse models of autism and schizophrenia[144,173].

Alzheimer disease. 2PCI experiments can be used as a direct and accurate approach to probe neuronal dysfunction in mouse models that mimic the pathology of Alzheimer disease. In such disease models, 2PCI makes it possible to correlate changes in the activity of single neurons with their proximity to amyloid plaques. Because one can longitudinally image neurons across several weeks, it is also possible to monitor the progression of their dysfunction, as well as their potential recovery after therapeutic interventions. Thus, previous 2PCI work has demonstrated that a dynamic imbalance in synaptic excitation and inhibition in pathologically disrupted brain circuits in mouse models of Alzheimer disease causes hyperactivity and hypoactivity in different subsets of neurons[174–176]. Furthermore, multicolour imaging suggested that this neuronal dysfunction was correlated with the amyloid-β burden in affected brain regions.

Stroke. Stroke is amongst the most common neurological disorders and is presently the leading cause of adult-onset disability worldwide[177]. Stroke pathology broadly occurs in two phases: an acute phase marked by ischaemia and cell death, and a chronic phase in which neural circuits reorganize and some recovery of function is possible. 2PCI has been used to gain mechanistic insights into both of these phases. Acutely after stroke, 2PCI has been used to record the time course and spatial extent of neuronal dysfunction[178,179], to test the roles of specific receptors in the propagation of cortical spreading depressions[180,181] and to quantify changes in $[Ca^{2+}]_i$ handling in non-neuronal cells such as astrocytes[178,180,182],

microglia[183,184] and pericytes[185]. In the weeks following stroke, 2PCI in the peri-infarct cortex has been used to investigate how sensory circuits change throughout recovery[186,187]. Coupled with cell type-specific expression of GECIs, 2PCI has also been used to test how changes in the activity of thalamocortical inputs[188] and vasoactive-intestinal polypeptide interneurons[189] contribute to recovery.

Non-neuronal cells

Not all calcium signals are related to action potential firing in neurons. Although the vast majority of 2PCI experiments in the brain have focused on electrically excitable neurons, intracellular calcium signalling is also essential for non-neuronal cells of the central nervous system. Amongst these cells, changes in $[Ca^{2+}]_i$ have been studied most extensively in astrocytes. In fact, because astrocytes are electrically non-excitable cells, electrophysiology is not a useful tool to understand their function. Astrocytes can also be visualized in vivo by injecting the dye sulforhodamine 101 (SR101), which selectively labels these glial cells[190,191]. More recently, AAVs and transgenic mouse lines have been generated to enable expression of high-sensitivity GECIs specifically in astrocytes[192,193], and software tools have been developed specifically for analysis of astrocyte calcium signals[194]. 2PCI has also been used to study calcium signalling in microglia[195,196], Müller glia of the retina[197] and vascular mural cells[198,199], although these areas are less well explored.

Reproducibility and data repositories

In the previous section, we provided examples of optimal quality of imaging and calcium traces. Unfortunately, storage and sharing of 2PCI data, or processing pipelines, are not standardized within and across laboratories. On the other hand, grassroots efforts initiated in individual laboratories have begun to provide resources to help standardize how 2PCI data are analysed, shared and deposited.

Data formats and repositories

The organization and reporting requirements for 2PCI data sets vary significantly depending on the funding source, publisher or collaboration consortium. In general, raw data from 2PCI are saved as multi-page .tiff files, although most commercial acquisition systems use different proprietary formats. These files often contain metadata information regarding acquisition and system parameters. After a preprocessing pipeline is executed to extract the activity of each ROI, downstream analyses are performed on the resulting multidimensional time series, which includes other parameters related to behaviour or stimuli. Neurodata Without Borders (NWB) provides a flexible framework to incorporate this and other critical information for each experiment (mouse age, sex and genetic strain, brain area, manipulation and so on) in a structured format. NWB can be considered the most widespread standard to store data sets and associated metadata, as well as the results of data analyses.

Data sets need to be stored for sharing or archiving purposes, which can then be a useful resource for

beginners in the field to compare their data sets. Several available solutions have been used for neurophysiology and 2PCI data, including Zenodo, DANDI, FigShare and CRCNS. Notably, some repositories also enable generating a DOI, and therefore become citable. Moreover, an increasing number of repositories provide application programming interfaces to efficiently download and upload data and/or associated metadata. An exemplary case is the Allen Brain Observatory repository, which contains a structured and organized set of recordings from GCaMP6-expressing neurons in selected cortical layers, visual areas and Cre lines[200]. Unfortunately, a single repository that is universally used for 2PCI does not yet exist.

Reproducibility of analysis pipelines

In order to completely reproduce results from other laboratories, it is not only necessary to access data sets with the appropriate meta-information but also to implement the same preprocessing and analysis steps, using the same version of software packages. Notable attempts to standardize and provide platforms for reproducible and scalable analysis of PCI data are DataJoint and Neuroscience Cloud Analysis As a Service (NeuroCAAS).

Minimum reporting standards

There is no universally agreed upon standard for reporting methods used in 2PCI experiments. At a minimum, investigators should include information on the experimental preparation, data acquisition hardware, imaging settings and data processing pipeline. Details pertinent for describing the experimental preparation include the specific calcium indicator used and selection criteria, how the indicator was delivered to cells of interest (including recombinant AAV serotype concentration, promoter and other relevant details), animal information (including age, sex and strain) and imaging preparation (including the type of cranial window used and timing relative to indicator delivery). As 2PCI microscopes can be highly customized, a description of acquisition hardware and imaging settings should include details on the type of laser used (wavelength, repetition rate, power at sample), scanning hardware (galvo/galvo, galvo/resonant, AODs and so on), imaging field of view (dimensions in pixels and micrometres), acquisition frame rate, microscope objective (including magnification and numerical aperture), emission filters and PMTs (including gain settings). For data processing, a full description of the analysis pipeline should be included, from raw data to final analysis. This might include any motion correction performed, preprocessing or filtering of data, spatial or temporal down-sampling, source localization/extraction methods, data normalization and spike inference method used, if applicable. If published algorithms are implemented, these should be cited, but specific parameters used for analysis should still be included, as these can be significantly customized in most cases. Any custom written code should be described in detail and made available through publicly accessible repositories such as GitHub.

Limitations and optimizations

Despite its enormous value in modern neuroscience, 2PCI does have significant shortcomings. In this section, we review limitations of this technique that currently preclude 2PCI from achieving single spike resolution, and other challenges for imaging deep structures or large fields of view. We also provide a list of optimizations and tricks of the trade that can counteract these limitations. Please refer to TABLE 2 for a list of frequent problems with 2PCI.

Garbage in, garbage out

In calcium imaging, the quality of the analysed results is only as good as the primary data collected. Unfortunately, with 2PCI, signals related to action potential firing are embedded in noisy calcium fluorescence traces. Several factors contribute to the noise, including the variable quality of the window preparation, problems with viral expression of the GECI, motion artefacts and shot noise (which comes from statistical fluctuations in how photons are detected by PMTs). Experimenters should take care to maximize the quality of the preparation, rejecting data sets in which the window clarity was compromised, in which GECI expression was either too low or too high, or in which excessive motion artefact could not be corrected.

Single spike detection

Resolving single spikes remains the greatest challenge for 2PCI. This is especially true for inhibitory interneurons and other neurons that fire in rapid bursts of action potentials. Initially, the limitation was in the scanning speed, but the use of resonant mirrors allowing for frame rates of 30 Hz (more than adequate for current GECIs) proved transformative for the field[85]. However, as each new generation of GECIs is engineered to have higher sensitivity and faster rise times/decays[23], it may someday be possible to achieve spike detection comparable with electrophysiology, provided we can scan the tissue faster. Until then, any strategies that provide greater imaging speed can be used to record more neurons. Other important techniques have been developed in recent years to rapidly image volumes of brain tissue (BOX 2). As discussed earlier, a simple strategy to increase image acquisition rates is to forego 2D scanning to achieve more efficient sampling of ROIs using targeted path scanning with standard galvos[201] or random-access multiphoton microscopy with AODs[81,202,203] (FIG. 4c). Unfortunately, AODs are costly, sensitive to the available laser power and require more complicated optics than standard resonant galvos[204,205]. Moreover, when arbitrary scanning patterns are used for in vivo 2PCI, movement artefacts cannot be corrected post hoc. Perhaps for these reasons, few groups presently use these methods for 2PCI.

Sub-threshold activity

Intracellular electrophysiology is the only viable technique to reliably record the small fluctuations in resting membrane potential (V_m) that are necessary to investigate sub-threshold synaptic inputs arriving at the soma or spontaneous depolarizations (up states) related to the simultaneous co-activation of neuronal ensembles in

Table 2 | **Limitations of 2PCI and optimizations**

Limitation	Cause	Optimization/workaround/solution
Poor detection of single spikes	Current GECIs have low sensitivity and have slow kinetics for binding Ca^{2+}	Develop better GECIs with faster rise times and decays, higher sensitivity
		Develop better voltage sensors (Supplementary Table 2)
	Current PMTs are not sensitive enough	Develop better photodetectors with greater quantum efficiency
	Slow raster scanning	Use targeted path scanning, resonant mirrors or AODs
		Scan smaller field of view
Imaging limited to small cortical area	Single area of raster scanning	Multiplexed scanning or dual-axis 2P microscopy
		Use lower magnification objective (typically at the cost of lower numerical aperture)
Imaging limited to superficial cortex; cannot image deep	Brain tissue greatly scatters excitation light (laser) and emitted photons resulting in poor signal at greater depths	GRIN lens
		Red-shifted GECIs
		3P imaging
		Adaptive optics
Limited to head-fixed behaviours	2P microscopes are large	Miniaturized head-mounted 2P microscopes
Poor dynamics in inhibitory interneurons	Because interneurons fire in high-frequency bursts, 2PCI cannot resolve individual spikes as well as in excitatory neurons that fire sparsely	Use caution when interpreting 2PCI data from interneurons, and consider using in vivo Ephys to confirm results
		Voltage imaging
Failure to detect dynamics in tonically active neurons	2PCI cannot detect decreases in firing of tonically active neurons	Voltage imaging
Poor image quality	Suboptimal cranial window	Reject windows with blood, bone growth, excessive motion artefact
	Poor GECI expression	Optimize viral expression
	Noisy image	Optimize laser power, PMT gain, frame averaging, alignment of laser
Epileptiform discharges	Widespread expression of GECIs with the tTA transactivator can be toxic to neurons, which leads them to adopt aberrant forms of synchronous activity	Avoid using certain transgenic lines of GCaMP mice, especially GCaMP6f, and lines driven by Emx1-Cre
Photodamage, including phototoxicity, bleaching, thermal injury	Prolonged scanning or high laser power	Reduce laser power, minimize scanning time (especially over a small field of view)
Filled-in cells	High GECI expression levels can cause some neurons to appear excessively bright and lack dynamic changes in fluorescence, which may indicate health problems	Avoid overexpressing GECI by using low virus titre and limit imaging to a narrow window of time post injection
		Use transgenic mice with stable expression

AOD, acousto-optical deflector; GECI, genetically encoded calcium indicator; GRIN, gradient refractive index; 2P, two-photon; 2PCI, two-photon calcium imaging; 3P, three-photon; PMT, photomultiplier tube.

the idling brain. Although 2P imaging of sub-threshold changes in V_m is possible with voltage sensors, further improvements will be necessary to improve their sensitivity and imperviousness to photobleaching for mainstream neuroscientists to adopt them (Supplementary Table 2). Still, the latest generations of voltage indicators, such as ASAP3 (REF.[206]), look very promising.

Studying neuronal inhibition using 2PCI remains difficult. Although hyperpolarization without any change in action potential firing has no effect on the calcium signal, decreases in action potential firing in tonically active neurons as a result of inhibition would appear as negative calcium signals in highly active neurons[207]. Of course, such dynamics are virtually undetectable in less active cells with low baseline fluorescence. In addition, the slower kinetics of certain GECIs might obscure such processes. Finally, even if detected, such negative calcium signals must be discriminated from motion artefacts, which might pose problems for some of the current analysis pipelines. In conclusion, examining inhibition using 2PCI requires, if at all possible, specific experimental and analytical strategies.

Recording from more neurons
Understanding brain function in health and disease necessitates the large-scale interrogation and monitoring of neuronal activity across different brain regions simultaneously. Ideally, this means recording from as many

Box 2 | Volume imaging

We discuss several approaches for two-photon calcium imaging (2PCI) in volumes of tissue (for a review, see REF.[255]). The simplest way is by moving the objective along its optical axis using a piezoelectric device[85] to multiple depths, with 2D raster scanning occurring at each axial position. However, the travel time for the objective to reach each axial position limits volume imaging to two or three planes when using a resonant–galvanometer-mounted mirror (galvo) system. Using fast piezoelectric devices, reasonable volume rates can be achieved over a small axial range (for example, three planes at 7.8 Hz (REF.[125]). Another strategy for volume imaging is to use tunable lenses or spatial light modulators to rapidly move the laser focus along the optical axis but without moving the objective. This avoids the problem posed by inertia but requires controlling the wavefront of the excitation light, because a focus shift axially relative to the objective corresponds to a change in the beam divergence. This has been used to image dendrites, somata and axons of hippocampal neurons in behaving mice[256].

Axially elongated foci, such as Bessel beams, generate projections of a volume at the rate of 2D images[257–259], effectively turning the microscope's frame rate into the volume acquisition rate. These and similar methods[260] rely on deliberately projecting multiple resolution elements into each measurement. As a result, these approaches sample space densely, providing benefits over random-access microscopy in specimens that move unpredictably — such as awake animals or moving particles — or when targets are challenging to select rapidly, such as dendritic spines. However, recovering sources from projected measurements requires either a spatially or a temporally sparse signal and/or computational methods to unmix the signal sources. In other words, although Bessel beam calcium imaging can in theory achieve single-cell resolution, in practice this is only true in very sparsely labelled tissue.

Light sheet microscopy
A fluorescence microscopy technique with optical sectioning capability in which the sample is illuminated perpendicularly to the direction of observation by a laser light sheet. Although light sheet microscopy is often used for calcium imaging of live zebrafish embryos, it is not discussed in detail in this Primer because it is technically not a form of two-photon calcium imaging.

Adaptive optics
Technology used to optimize the performance of optical systems by reducing distortions of the incoming wavefront of light using deformable mirrors. In two-photon microscopy, it helps correct for aberrations due to inhomogeneities in the biological specimen.

neurons as possible in behaving animals. One of the limitations of conventional 2PCI is that scanning is limited to a single imaging plane, which in mouse neocortex translates to ~200 neurons. Considering how the optimal image acquisition speed for current GECIs is ~15 Hz, any additional speed provided by the latest technologies developed for faster scanning can be used to record from more neurons (in depth or along a single plane).

Recent studies combining calcium imaging with light sheet microscopy have recorded from thousands of neurons in larval zebrafish[208]. One strategy is to build custom optical systems for 2PCI that provide larger fields of view for mesoscopic 2PCI[209–211]. For example, a completely custom 2P imaging system expanded the field of view >50 times compared with commercial systems[210]. A different approach is to increase speed by splitting up the excitation beam to generate multiple excitation foci that are scanned simultaneously across the sample. This spatio-temporal multiplexing uses two or more temporally multiplexed foci for simultaneous imaging in adjacent fields of view in a single imaging plane or multiple focal planes[83,212]. This permits fluorescence from spatially distinct beams to be distinguished because fluorescence detected at different times is assigned to different portions of the image or different axial planes[83,213–217] (FIG. 4d). An essential condition is that the fluorescence lifetime of the calcium indicator (typically in the nanosecond range) is shorter than the laser repetition periods (tens of nanoseconds). Using lasers with a lower repetition rate (a few megahertz) could further increase the number of neurons recorded. Recently, light beads microscopy achieved single-cell 2PCI for volumes of ~3 × 5 × 0.5 mm³ in mouse neocortex at ~5 Hz using 30 spatially and temporally separated foci[216]. However, in preparations where scattering is minimal, such as the larval zebrafish or *Hydra vulgaris*, the

spatio-temporal trade-off associated with point scanning microscopy can be obviated using more efficient illumination approaches such as a light sheet, SCAPE, wide field or light field[218].

Non-invasive deep tissue 2PCI
An important limitation of 2PCI is that one cannot image deep into brain tissue due to light scattering of the excitation laser light and of the emitted fluorescence, which degrades image quality[76,77,219]. As a result, 2PCI has mainly been used to record from superficial cortical neurons in lissencephalic mammalian brains, such as those of mice, rats or marmosets[220]. A few optimizations exist to use 2PCI to record from deeper brain regions. Despite some advantages of more invasive methods such as micro-endoscopy with GRIN lenses, for specific applications (for example, imaging below the corpus callosum) there are less invasive alternatives for 2PCI of the entire cortical thickness. The first is the use of adaptive optics (FIG. 4b), which aims to correct aberrations introduced by biological specimens that distort the laser pulse and decrease the efficiency of excitation[221–223]. These aberrations become increasingly more prominent with increasing depth[224]. In the case of 2PCI, wavefront optimization with adaptive optics has been used to characterize the tuning properties of thalamic boutons deep in mouse primary visual cortex[225]. Another approach is the use of regenerative laser amplifiers, which yield laser pulses with higher photon density — increasing the probability of the two-photon effect — but at a lower repetition rate. 2PCI with regenerative amplifiers was used to record sensory evoked signals from somata of layer 5 pyramidal neurons[226]. Present limitations of this technique are the lack of wavelength tunability and the slower speed of imaging. Three-photon (3P) excitation, which uses longer excitation wavelengths (>1,300 nm), can further increase the imaging depth because of reduced scattering at these longer wavelengths and thanks to background suppression by higher-order non-linear excitation[227]. However, it suffers from similar drawbacks to regenerative amplifiers[228]. 3P imaging has been used to probe neural activity nearly 1 mm deep in the hippocampus of adult mice[229]. Even more remarkable feats of deep imaging can be achieved by combining 3P microscopy and adaptive optics[230]. Combining 2P and 3P imaging was also used to simultaneously monitor network activity in cortical and subcortical regions in mice[231]. Related to deep tissue 2PCI is the notion of volume imaging, which is discussed in more detail in BOX 2.

Recordings in freely moving mice
Although 2PCI is well suited for recordings in head-fixed animals engaged in decision-making or navigational tasks, conventional 2P microscopes are not compatible with calcium imaging in freely moving mice. As a result, neuroscientists in recent years could only turn to silicon probes and portable one-photon mini-scopes to record activity in freely moving mice. Fortunately, the technology for head-mounted miniaturized 2P scopes (originally developed nearly two decades ago[69]) has undergone significant improvements in recent years[232]. Considering the superior cellular resolution and optical sectioning of

2P scopes compared with one-photon mini-scopes, 2PCI could become the preferred method for probing neural activity in freely moving mice in the very near future.

Real-time analysis during imaging

Even though calcium imaging has enabled unprecedented access to the activity of large brain areas at high spatial and temporal resolution, the size and complexity of imaging data sets have created a serious bottleneck in the analysis pipelines and, consequently, have slowed the experiment–analysis–theory cycle[233]. For instance, visual inspection by experimenters during imaging is not sufficient to assess the quality of collected data and the nature of spatio-temporal neural patterns, making it impossible to gather feedback on ongoing experiments or to adaptively tune experimental settings and parameters. As a result, laboratories are exposed to huge opportunity and economic costs. To overcome such challenges, recent analysis approaches operate on streams of data (frame by frame or mini-batches of frames)[234]. Such approaches enable real-time analysis and closed-loop experiments, while helping significantly reduce the computational and memory footprints in the analysis of very large data sets. Examples of such modalities are all-optical experiments combining calcium imaging and optogenetics[235], closed-loop experiments[164] and brain–computer interfaces[236]. Besides closed-loop applications, these algorithms also enable gathering feedback during or shortly after an experiment, and provide the substrate to optimize adaptive experimental design.

Outlook

The future of 2PCI is bright. The lower cost of lasers and microscopes, the improvement of GECIs in recent years, the availability of transgenic animals that express GECIs and the development of user-friendly tools for data analysis have made it possible for an ever-growing number of scientists to incorporate 2PCI in their experiments. In the near future, we can anticipate changes in four aspects of 2PCI: advances in GECIs; improvements in hardware and software, especially in machine learning algorithms to analyse calcium signals; an expansion of resources for standardization of 2PCI analysis pipelines; and combined applications of 2PCI with in vivo electrophysiology in behaving animals.

It is almost certain that in the next few years we will witness the development of new and improved GECIs. Improvements in their sensitivity that can greatly impact the signal-to-noise ratio will aid in imaging larger brain volumes because they will permit shorter dwell times and faster sampling. Furthermore, the development of GECIs with faster kinetics and increased linearity in action potential detection will benefit the study of neurons that fire quickly or in bursts, such as interneurons. Engineering other indicators with an excitation spectrum pushed further into the infrared band (>1,040 nm) will enable 2PCI at greater depths by causing less scattering for both excitation and emission light and by causing less signal loss from absorption by haemoglobin. These will be welcome advances. However, population recordings with 2PCI provide only an indirect read-out of the action potential firing of neurons and cannot assess sub-threshold activity. Thus, there are opportunities for more direct reporters of activity, including indicators of voltage changes[206,237–240] or neurotransmitter release[241,242].

Naturally, the design of better calcium and voltage sensors will motivate engineers to develop better hardware to sample the brain more quickly. Thus, we can expect progress in technologies capable of faster 3D imaging[243]. Other advances in hardware will allow for 3P imaging, adaptive optics and the use of GRIN lenses to become more mainstream. This will permit in vivo 2PCI studies to extend rapidly beyond the currently targeted cortical areas to neurons in deeper brain regions. In parallel, it is certain that miniaturized 2P microscopes for use in freely moving animals[70] will be rapidly disseminated.

On the software side, we can expect changes in two areas. First, the development of robust data analysis tools is of the utmost importance, as the acquired 2PCI data sets will only increase further in sheer size and complexity. Especially challenging are large-scale volumetric data sets, producing data at rates that can easily surpass 1 TB per hour. At the present time, the cost and complexity associated with the storage and analysis of such data sets, respectively, could hinder the democratization and widespread adoption of 2PCI by the community[244]. Indeed, it is conceivable that analysis of single data sets might require days to complete. Second, other developments are needed for streaming or mini-batch analysis algorithms[97]. These would not only facilitate closed-loop and all-optical experiments (jointly with optogenetics[245]) but also provide immediate feedback on ongoing experiments and improve scalability. The use of GPUs is a promising avenue to exploit machine learning hardware and software developments that can significantly speed up analyses[246] or the development of advanced brain–computer interfaces. Although some recent research is focusing on building brain–computer interfaces with calcium imaging[151], the performance is still limited because of a lack in speed and precision in extracting neural activity[246].

We live in a world of machine learning and, of course, it plays a key role in 2PCI. As newer GECIs improve spike detection, deep learning methods open the path to novel calibration algorithms at the single-neuron level[124]. Meanwhile, emerging all-optical methods[247] can causally elicit single spikes and help parameterize, on the fly, inverse models to deconvolve fluorescence signals. Requiring a minimal amount of data, these algorithms could precisely quantify the uncertainty in spike inference for each neuron. Computational models specific for different neuron types could then improve the performance of deconvolution algorithms used to infer action potential firing from calcium signals. The generation of large data sets containing both electrophysiological and 2PCI data remains of vital importance[5,124], because this will reduce false negatives during analysis by providing ground truth data. Relatedly, powerful machine learning approaches that exploit synergies among neurons across trials to increase the fidelity and temporal resolution of extracted spikes have shown very promising results in decoding behaviour[248].

Moreover, as the application of machine learning in calcium imaging analysis matures, a higher level of automation and throughput for analysis tasks can be expected to follow. This will be enabled by more generalized and robust machine learning models. The barrier to training and deploying these methods will also eventually disappear as more research is devoted to how to use smaller training data sets. Software packages that realistically simulate calcium imaging movies[120] will play a prominent role in training these algorithms and in evaluating the preprocessing packages on equal footing. Extensive collaborative experimental efforts, such as the International Brain Laboratory or the IARPA MICrONS project, require high-quality automated analysis pipelines to benefit the scientific community.

Standardization is a commendable effort that the community is pursuing, but the landscape remains somewhat fragmented. Indeed, reproducing or building upon results across laboratories is an arduous task. Theorists, in particular, face significant barriers in accessing and interpreting data sets from 2PCI. We envisage either the emergence of a few widely adopted standard frameworks (such as NWB, DANDI or DataJoint) or the establishment of meta-frameworks able to intelligently aggregate information from multiple sources, while at the same time offering convenient application programming interfaces to incrementally load and save sections of data sets or the associated meta-information.

Electrophysiologists may view the development of Neuropixels probes[249,250] as a major threat to 2PCI because they are designed to record action potential firing in thousands of neurons, across multiple brain regions and depths, in awake behaving animals. We see the emergence of silicon probes as an opportunity for combining the two technologies. To this end, the probes are already small enough for chronic implantations in mice[146], which minimizes geometric limitations for combined electrophysiology and microscopy experiments. These combined recordings would serve to improve and test both extracellular spike sorting and deconvolution algorithms, and thereby reduce the bias associated with either technique separately[5]. Moreover, one could potentially match genetically identified neuron subtypes with their extracellular waveforms from high-density probes. Regardless, at the single-cell level, 2PCI will remain an essential tool for studying the mechanisms associated with synaptic function and synaptic plasticity in genetically identified cell classes. Although with silicon probes one can determine the cell type using opto-tagging[251], this is more cumbersome and less scalable than using 2PCI. Furthermore, 2PCI studies combined with targeted perturbations of neuronal signalling proteins can provide highly quantitative information on the intracellular mechanisms involving calcium signalling in specific neuronal subdomains, such as dendritic spines and axon terminals. In combination with optogenetics, such studies will contribute to a better understanding of local network function. This goal will also require the development of defined animal behaviours that can be combined with 2PCI, as this technique is so amenable to head-fixed experimentation[252]. A final, yet vital, area likely to expand in the coming years is 2PCI in animal model systems other than mice, especially non-human primates[253] because of the greater similarity of their brains to those of humans and their ability to engage in more elaborate behavioural tasks. In sum, there has never been a better time to embark on 2PCI experiments.

1. Grewe, B. F. & Helmchen, F. Optical probing of neuronal ensemble activity. *Curr. Opin. Neurobiol.* **19**, 9042–9052 (2009).
2. Lecoq, J., Orlova, N. & Grewe, B. F. Wide. Fast. Deep: recent advances in multiphoton microscopy of in vivo neuronal activity. *J. Neurosci.* **39**, 9042–9052 (2019).
3. Gobel, W. & Helmchen, F. In vivo calcium imaging of neural network function. *Physiology* **22**, 358–365 (2007).
4. Grienberger, C. & Konnerth, A. Imaging calcium in neurons. *Neuron* **73**, 862–885 (2012).
5. Wei, Z. et al. A comparison of neuronal population dynamics measured with calcium imaging and electrophysiology. *PLoS Comput. Biol.* **16**, e1008198 (2020).
6. Wilt, B. A. et al. Advances in light microscopy for neuroscience. *Annu. Rev. Neurosci.* **32**, 435–506 (2009).
7. Kondo, M., Kobayashi, K., Ohkura, M., Nakai, J. & Matsuzaki, M. Two-photon calcium imaging of the medial prefrontal cortex and hippocampus without cortical invasion. *eLife* **6**, e26839 (2017).
8. Grynkiewicz, G., Poenie, M. & Tsien, R. Y. A new generation of Ca²⁺ indicators with greatly improved fluorescence properties. *J. Biol. Chem.* **260**, 3440–3450 (1985).
9. Tsien, R. Y. New calcium indicators and buffers with high selectivity against magnesium and protons: design, synthesis, and properties of prototype structures. *Biochemistry* **19**, 2396–2404 (1980).
10. Paredes, R. M., Etzler, J. C., Watts, L. T., Zheng, W. & Lechleiter, J. D. Chemical calcium indicators. *Methods* **46**, 143–151 (2008).
11. Helmchen, F., Borst, J. G. & Sakmann, B. Calcium dynamics associated with a single action potential in a CNS presynaptic terminal. *Biophys. J.* **72**, 1458–1471 (1997).

12. Garaschuk, O., Milos, R. & Konnerth, A. Targeted bulk-loading of fluorescent indicators for two-photon brain imaging in vivo. *Nat. Protoc.* **1**, 380–386 (2006).
13. Golshani, P. & Portera-Cailliau, C. In vivo 2-photon calcium imaging in layer 2/3 of mice. *J. Vis. Exp.* https://doi.org/10.3791/681 (2008).
14. Tsien, R. Y. The green fluorescent protein. *Annu. Rev. Biochem.* **67**, 509–544 (1998).
15. Mank, M. & Griesbeck, O. Genetically encoded calcium indicators. *Chem. Rev.* **108**, 1550–1564 (2008).
16. Lutcke, H. et al. Optical recording of neuronal activity with a genetically-encoded calcium indicator in anesthetized and freely moving mice. *Front. Neural Circuits* **4**, 9 (2010).
17. Looger, L. L. & Griesbeck, O. Genetically encoded neural activity indicators. *Curr. Opin. Neurobiol.* **22**, 18–23 (2012).
18. Tian, L., Akerboom, J., Schreiter, E. R. & Looger, L. L. Neural activity imaging with genetically encoded calcium indicators. *Prog. Brain Res.* **196**, 79–94 (2012).
19. Miyawaki, A. et al. Fluorescent indicators for Ca²⁺ based on green fluorescent proteins and calmodulin. *Nature* **388**, 882–887 (1997).
20. Mank, M. et al. A genetically encoded calcium indicator for chronic in vivo two-photon imaging. *Nat. Methods* **5**, 805–811 (2008).
21. Baird, G. S., Zacharias, D. A. & Tsien, R. Y. Circular permutation and receptor insertion within green fluorescent proteins. *Proc. Natl Acad. Sci. USA* **96**, 11241–11246 (1999).
22. Nakai, J., Ohkura, M. & Imoto, K. A high signal-to-noise Ca²⁺ probe composed of a single green fluorescent protein. *Nat. Biotechnol.* **19**, 137–141 (2001).
23. Zhang, Y. et al. Fast and sensitive GCaMP calcium indicators for imaging neural populations. Preprint at *bioRxiv* https://doi.org/10.1101/2021.11.08.467793 (2021).

24. Dana, H. et al. Sensitive red protein calcium indicators for imaging neural activity. *eLife* **5**, e12727 (2016).
25. Inoue, M. et al. Rational engineering of XCaMPs, a multicolor GECI suite for in vivo imaging of complex brain circuit dynamics. *Cell* **177**, 1346–1360.e24 (2019).
26. Mohr, M. A. et al. jYCaMP: an optimized calcium indicator for two-photon imaging at fiber laser wavelengths. *Nat. Methods* **17**, 694–697 (2020).
27. Shemesh, O. A. et al. Precision calcium imaging of dense neural populations via a cell-body-targeted calcium indicator. *Neuron* **107**, 470–486.e11 (2020).
28. Chen, Y. et al. Soma-targeted imaging of neural circuits by ribosome tethering. *Neuron* **107**, 454–469.e6 (2020).
29. Broussard, G. J. et al. In vivo measurement of afferent activity with axon-specific calcium imaging. *Nat. Neurosci.* **21**, 1272–1280 (2018).
30. Lacefield, C. O., Pnevmatikakis, E. A., Paninski, L. & Bruno, R. M. Reinforcement learning recruits somata and apical dendrites across layers of primary sensory cortex. *Cell Rep.* **26**, 2000–2008.e2 (2019).
31. Lee, K. S., Vandemark, K., Mezey, D., Shultz, N. & Fitzpatrick, D. Functional synaptic architecture of callosal inputs in mouse primary visual cortex. *Neuron* **101**, 421–428.e5 (2019).
32. Keiser, M. S., Chen, Y. H. & Davidson, B. L. Techniques for intracranial stereotaxic injections of adeno-associated viral vectors in adult mice. *Curr. Protoc. Mouse Biol.* **8**, e57 (2018).
33. He, C. X., Arroyo, E. D., Cantu, D. A., Goel, A. & Portera-Cailliau, C. A versatile method for viral transfection of calcium indicators in the neonatal mouse brain. *Front. Neural Circuits* **12**, 56 (2018).
34. Aschauer, D. F., Kreuz, S. & Rumpel, S. Analysis of transduction efficiency, tropism and axonal transport of AAV serotypes 1, 2, 5, 6, 8 and 9 in the mouse brain. *PLoS ONE* **8**, e76310 (2013).

35. Graybuck, L. T. et al. Enhancer viruses for combinatorial cell-subclass-specific labeling. *Neuron* **109**, 1449–1464.e13 (2021).

36. Mich, J. K. et al. Functional enhancer elements drive subclass-selective expression from mouse to primate neocortex. *Cell Rep.* **34**, 108754 (2021).

37. Haery, L. et al. Adeno-associated virus technologies and methods for targeted neuronal manipulation. *Front. Neuroanat.* **13**, 93 (2019).

38. Daigle, T. L. et al. A suite of transgenic driver and reporter mouse lines with enhanced brain-cell-type targeting and functionality. *Cell* **174**, 465–480.e22 (2018).

39. Challis, R. C. et al. Systemic AAV vectors for widespread and targeted gene delivery in rodents. *Nat. Protoc.* **14**, 379–414 (2019).

40. Mathiesen, S. N., Lock, J. L., Schoderboeck, L., Abraham, W. C. & Hughes, S. M. CNS transduction benefits of AAV-PHP.eB over AAV9 are dependent on administration route and mouse strain. *Mol. Ther. Methods Clin. Dev.* **19**, 447–458 (2020).

41. Chen, T. W. et al. Ultrasensitive fluorescent proteins for imaging neuronal activity. *Nature* **499**, 295–300 (2013).

42. Tian, L. et al. Imaging neural activity in worms, flies and mice with improved GCaMP calcium indicators. *Nat. Methods* **6**, 875–881 (2009).

43. Dana, H. et al. Thy1-GCaMP6 transgenic mice for neuronal population imaging in vivo. *PLoS ONE* **9**, e108697 (2014).

44. Madisen, L. et al. Transgenic mice for intersectional targeting of neural sensors and effectors with high specificity and performance. *Neuron* **85**, 942–958 (2015).

45. Steinmetz, N. A. et al. Aberrant cortical activity in multiple GCaMP6-expressing transgenic mouse lines. *eNeuro* **4**, ENEURO.0207-17.2017 (2017).

46. Holtmaat, A. et al. Long-term, high-resolution imaging in the mouse neocortex through a chronic cranial window. *Nat. Protoc.* **4**, 1128–1144 (2009).

47. Yang, G., Pan, F., Parkhurst, C. N., Grutzendler, J. & Gan, W. B. Thinned-skull cranial window technique for long-term imaging of the cortex in live mice. *Nat. Protoc.* **5**, 201–208 (2010).

48. Xu, H. T., Pan, F., Yang, G. & Gan, W. B. Choice of cranial window type for in vivo imaging affects dendritic spine turnover in the cortex. *Nat. Neurosci.* **10**, 549–551 (2007).

49. Isshiki, M. & Okabe, S. Evaluation of cranial window types for in vivo two-photon imaging of brain microstructures. *Microscopy* **63**, 53–63 (2014).

50. Mostany, R. & Portera-Cailliau, C. A craniotomy surgery procedure for chronic brain imaging. *J. Vis. Exp.* https://doi.org/10.3791/680 (2008).

51. Ghanbari, L. et al. Cortex-wide neural interfacing via transparent polymer skulls. *Nat. Commun.* **10**, 1500 (2019).

52. Pak, N. et al. Closed-loop, ultraprecise, automated craniotomies. *J. Neurophysiol.* **113**, 3943–3953 (2015).

53. Kim, T. H. et al. Long-term optical access to an estimated one million neurons in the live mouse cortex. *Cell Rep.* **17**, 3385–3394 (2016).

54. Heo, C. et al. A soft, transparent, freely accessible cranial window for chronic imaging and electrophysiology. *Sci. Rep.* **6**, 27818 (2016).

55. Low, R. J., Gu, Y. & Tank, D. W. Cellular resolution optical access to brain regions in fissures: imaging medial prefrontal cortex and grid cells in entorhinal cortex. *Proc. Natl Acad. Sci. USA* **111**, 18739–18744 (2014).

56. Andermann, M. L. et al. Chronic cellular imaging of entire cortical columns in awake mice using microprisms. *Neuron* **80**, 900–913 (2013).

57. El-Boustani, S. et al. Anatomically and functionally distinct thalamocortical inputs to primary and secondary mouse whisker somatosensory cortices. *Nat. Commun.* **11**, 3342 (2020).

58. Mizrahi, A., Crowley, J. C., Shtoyerman, E. & Katz, L. C. High-resolution in vivo imaging of hippocampal dendrites and spines. *J. Neurosci.* **24**, 3147–3151 (2004).

59. Velasco, M. G. & Levene, M. J. In vivo two-photon microscopy of the hippocampus using glass plugs. *Biomed. Opt. Express* **5**, 1700–1708 (2014).

60. Geiller, T. et al. Local circuit amplification of spatial selectivity in the hippocampus. *Nature* **601**, 105–109 (2022).

61. Howe, M. W. & Dombeck, D. A. Rapid signalling in distinct dopaminergic axons during locomotion and reward. *Nature* **535**, 505–510 (2016).

62. Barretto, R. P., Messerschmidt, B. & Schnitzer, M. J. In vivo fluorescence imaging with high-resolution microlenses. *Nat. Methods* **6**, 511–512 (2009).

63. Adelsberger, H., Garaschuk, O. & Konnerth, A. Cortical calcium waves in resting newborn mice. *Nat. Neurosci.* **8**, 988–990 (2005).

64. Grienberger, C. et al. Sound-evoked network calcium transients in mouse auditory cortex in vivo. *J. Physiol.* **590**, 899–918 (2012).

65. Meng, G. et al. High-throughput synapse-resolving two-photon fluorescence microendoscopy for deep-brain volumetric imaging in vivo. *eLife* **8**, e40805 (2019).

66. Otis, J. M. et al. Prefrontal cortex output circuits guide reward seeking through divergent cue encoding. *Nature* **543**, 103–107 (2017).

67. Jennings, J. H. et al. Interacting neural ensembles in orbitofrontal cortex for social and feeding behaviour. *Nature* **565**, 645–649 (2019).

68. Antonini, A. et al. Extended field-of-view ultrathin microendoscopes for high-resolution two-photon imaging with minimal invasiveness. *eLife* **9**, e58882 (2020).

69. Flusberg, B. A., Jung, J. C., Cocker, E. D., Anderson, E. P. & Schnitzer, M. J. In vivo brain imaging using a portable 3.9 gram two-photon fluorescence microendoscope. *Opt. Lett.* **30**, 2272–2274 (2005).

70. Zong, W. et al. Miniature two-photon microscopy for enlarged field-of-view, multi-plane and long-term brain imaging. *Nat. Methods* **18**, 46–49 (2021).

71. Zhao, Y. J. et al. Skull optical clearing window for in vivo imaging of the mouse cortex at synaptic resolution. *Light. Sci. Appl.* **7**, 17153 (2018).

72. Denk, W., Strickler, J. H. & Webb, W. W. Two-photon laser scanning fluorescence microscopy. *Science* **248**, 73–76 (1990).

73. Svoboda, K. & Yasuda, R. Principles of two-photon excitation microscopy and its applications to neuroscience. *Neuron* **50**, 823–839 (2006).

74. Denk, W. et al. Anatomical and functional imaging of neurons using 2-photon laser scanning microscopy. *J. Neurosci. Methods* **54**, 151–162 (1994).

75. Oheim, M., Beaurepaire, E., Chaigneau, E., Mertz, J. & Charpak, S. Two-photon microscopy in brain tissue: parameters influencing the imaging depth. *J. Neurosci. Methods* **111**, 29–37 (2001).

76. Helmchen, F. & Denk, W. Deep tissue two-photon microscopy. *Nat. Methods* **2**, 932–940 (2005).

77. Andresen, V. et al. Infrared multiphoton microscopy: subcellular-resolved deep tissue imaging. *Curr. Opin. Biotechnol.* **20**, 54–62 (2009).

78. Kobat, D. et al. Deep tissue multiphoton microscopy using longer wavelength excitation. *Opt. Express* **17**, 13354–13364 (2009).

79. Condylis, C. et al. Dense functional and molecular readout of a circuit hub in sensory cortex. *Science* **375**, eabl5981 (2022).

80. Gobel, W., Kampa, B. M. & Helmchen, F. Imaging cellular network dynamics in three dimensions using fast 3D laser scanning. *Nat. Methods* **4**, 73–79 (2007).

81. Duemani Reddy, G., Kelleher, K., Fink, R. & Saggau, P. Three-dimensional random access multiphoton microscopy for functional imaging of neuronal activity. *Nat. Neurosci.* **11**, 713–720 (2008).

82. Nadella, K. M. et al. Random-access scanning microscopy for 3D imaging in awake behaving animals. *Nat. Methods* **13**, 1001–1004 (2016).

83. Cheng, A., Gonçalves, J. T., Golshani, P., Arisaka, K. & Portera Cailliau, C. Simultaneous two-photon calcium imaging at different depths with spatiotemporal multiplexing. *Nat. Methods* **8**, 139–142 (2011).

84. Pnevmatikakis, E. A. et al. Simultaneous denoising, deconvolution, and demixing of calcium imaging data. *Neuron* **89**, 285–299 (2016).

85. Callamaras, N. & Parker, I. Construction of a confocal microscope for real-time $x−y$ and $x−z$ imaging. *Cell Calcium* **26**, 271–279 (1999).

86. Bonin, V., Histed, M. H., Yurgenson, S. & Reid, R. C. Local diversity and fine-scale organization of receptive fields in mouse visual cortex. *J. Neurosci.* **31**, 18506–18521 (2011).

87. Jia, H., Rochefort, N. L., Chen, X. & Konnerth, A. Dendritic organization of sensory input to cortical neurons in vivo. *Nature* **464**, 1307–1312 (2010).

88. Fan, G. Y. et al. Video-rate scanning two-photon excitation fluorescence microscopy and ratio imaging with cameleons. *Biophys. J.* **76**, 2412–2420 (1999).

89. Grienberger, C., Chen, X. & Konnerth, A. NMDA receptor-dependent multidendrite Ca^{2+} spikes required for hippocampal burst firing in vivo. *Neuron* **81**, 1274–1281 (2014).

90. Nguyen, Q. T., Callamaras, N., Hsieh, C. & Parker, I. Construction of a two-photon microscope for video-rate Ca^{2+} imaging. *Cell Calcium* **30**, 383–393 (2001).

91. Dombeck, D. A., Khabbaz, A. N., Collman, F., Adelman, T. L. & Tank, D. W. Imaging large-scale neural activity with cellular resolution in awake, mobile mice. *Neuron* **56**, 43–57 (2007).

92. Goldey, G. J. et al. Removable cranial windows for long-term imaging in awake mice. *Nat. Protoc.* **9**, 2515–2538 (2014).

93. Chen, J. L., Pfaffli, O. A., Voigt, F. F., Margolis, D. J. & Helmchen, F. Online correction of licking-induced brain motion during two-photon imaging with a tunable lens. *J. Physiol.* **591**, 4689–4698 (2013).

94. Podgorski, K. & Ranganathan, G. Brain heating induced by near-infrared lasers during multiphoton microscopy. *J. Neurophysiol.* **116**, 1012–1023 (2016).

95. Picot, A. et al. Temperature rise under two-photon optogenetic brain stimulation. *Cell Rep.* **24**, 1243–1253.e5 (2018).

96. Pachitariu, M. et al. Suite2p: beyond 10,000 neurons with standard two-photon microscopy. Preprint at *bioRxiv* https://doi.org/10.1101/061507 (2017).

97. Giovannucci, A. et al. CaImAn an open source tool for scalable calcium imaging data analysis. *eLife* **8**, e38173 (2019).

98. Cantu, D. A. et al. EZcalcium: open-source toolbox for analysis of calcium imaging data. *Front. Neural Circuits* **14**, 25 (2020).

99. Benisty, H., Song, A., Mishne, G. & Charles, A. Data processing of functional optical microscopy for neuroscience. Preprint at https://doi.org/10.48550/arXiv.2201.03537 (2022).

100. Pnevmatikakis, E. A. Analysis pipelines for calcium imaging data. *Curr. Opin. Neurobiol.* **55**, 15–21 (2019).

101. Stringer, C. & Pachitariu, M. Computational processing of neural recordings from calcium imaging data. *Curr. Opin. Neurobiol.* **55**, 22–31 (2019).

102. Hurwitz, C., Kudryashova, N., Onken, A. & Hennig, M. H. Building population models for large-scale neural recordings: opportunities and pitfalls. *Curr. Opin. Neurobiol.* **70**, 64–73 (2021).

103. Greenberg, D. S. & Kerr, J. N. Automated correction of fast motion artifacts for two-photon imaging of awake animals. *J. Neurosci. Methods* **176**, 1–15 (2009).

104. Guizar-Sicairos, M., Thurman, S. T. & Fienup, J. R. Efficient subpixel image registration algorithms. *Opt. Lett.* **33**, 156–158 (2008).

105. Pnevmatikakis, E. A. & Giovannucci, A. NoRMCorre: an online algorithm for piecewise rigid motion correction of calcium imaging data. *J. Neurosci. Methods* **291**, 83–94 (2017).

106. Dubbs, A., Guevara, J. & Yuste, R. moco: fast motion correction for calcium imaging. *Front. Neuroinform.* **10**, 6 (2016).

107. Lagache, T., Hanson, A., Perez-Ortega, J. E., Fairhall, A. & Yuste, R. Tracking calcium dynamics from individual neurons in behaving animals. *PLoS Comput. Biol.* **17**, e1009432 (2021).

108. Akemann, W. et al. Fast optical recording of neuronal activity by three-dimensional custom-access serial holography. *Nat. Methods* **19**, 100–110 (2022).

109. Buchanan, E. et al. Penalized matrix decomposition for denoising, compression, and improved demixing of functional imaging data. Preprint at *bioRxiv* https://doi.org/10.1101/334706 (2019).

110. Lecoq, J. et al. Removing independent noise in systems neuroscience data using DeepInterpolation. *Nat. Methods* **18**, 1401–1408 (2021).

111. Apthorpe, N. et al. in *Advances in Neural Information Processing Systems, Annual Conference on Neural Information Processing Systems* 3270–3278 (NIPS, 2016).

112. Soltanian-Zadeh, S., Sahingur, K., Blau, S., Gong, Y. & Farsiu, S. Fast and robust active neuron segmentation in two-photon calcium imaging using spatiotemporal deep learning. *Proc. Natl Acad. Sci. USA* **116**, 8554–8563 (2019).

113. Pachitariu, M. et al. in *Advances in Neural Information Processing Systems* 1745–1753 (NIPS, 2013).

114. Diego, F. & Hamprecht, F. in *Advances in Neural Information Processing Systems* 64–72 (NIPS, 2014).

115. Reynolds, S. et al. ABLE: an activity-based level set segmentation algorithm for two-photon calcium imaging data. *eNeuro* **4**, ENEURO.0012-17.2017 (2017).

116. Spaen, Q. et al. HNCcorr: a novel combinatorial approach for cell identification in calcium-imaging movies. *eNeuro* **6**, ENEURO.0304-18.2019 (2019).

117. Sheintuch, L. et al. Tracking the same neurons across multiple days in Ca^{2+} imaging data. *Cell Rep.* **21**, 1102–1115 (2017).

118. Mukamel, E. A., Nimmerjahn, A. & Schnitzer, M. J. Automated analysis of cellular signals from large-scale calcium imaging data. *Neuron* **63**, 747–760 (2009).
119. Helmchen, F. Calibration of fluorescent calcium indicators. *Cold Spring Harb. Protoc.* **2011**, 923–930 (2011).
120. Song, A., Gauthier, J. L., Pillow, J. W., Tank, D. W. & Charles, A. S. Neural anatomy and optical microscopy (NAOMi) simulation for evaluating calcium imaging methods. *J. Neurosci. Methods* **358**, 109173 (2021).
121. Berens, P. et al. Community-based benchmarking improves spike rate inference from two-photon calcium imaging data. *PLoS Comput. Biol.* **14**, e1006157 (2018).
122. Friedrich, J. & Paninski, L. in *Advances In Neural Information Processing Systems* 1984–1992 (NIPS, 2016).
123. Deneux, T. et al. Accurate spike estimation from noisy calcium signals for ultrafast three-dimensional imaging of large neuronal populations in vivo. *Nat. Commun.* **7**, 12190 (2016).
124. Rupprecht, P. et al. A database and deep learning toolbox for noise-optimized, generalized spike inference from calcium imaging. *Nat. Neurosci.* **24**, 1324–1337 (2021).
125. Peron, S. P., Freeman, J., Iyer, V., Guo, C. & Svoboda, K. A cellular resolution map of barrel cortex activity during tactile behavior. *Neuron* **86**, 783–799 (2015).
126. Kerr, J. N. et al. Spatial organization of neuronal population responses in layer 2/3 of rat barrel cortex. *J. Neurosci.* **27**, 13316–13328 (2007).
127. Golshani, P. et al. Internally mediated developmental desynchronization of neocortical network activity. *J. Neurosci.* **29**, 10890–10899 (2009).
128. Margolis, D. J. et al. Reorganization of cortical population activity imaged throughout long-term sensory deprivation. *Nat. Neurosci.* **15**, 1539–1546 (2012).
129. Musall, S. et al. Tactile frequency discrimination is enhanced by circumventing neocortical adaptation. *Nat. Neurosci.* **17**, 1567–1573 (2014).
130. He, C. X. et al. Tactile defensiveness and impaired adaptation of neuronal activity in the Fmr1 knock-out mouse model of autism. *J. Neurosci.* **37**, 6475–6487 (2017).
131. Chen, J. L., Carta, S., Soldado-Magraner, J., Schneider, B. L. & Helmchen, F. Behaviour-dependent recruitment of long-range projection neurons in somatosensory cortex. *Nature* **499**, 336–340 (2013).
132. Urai, A. E., Doiron, B., Leifer, A. M. & Churchland, A. K. Large-scale neural recordings call for new insights to link brain and behavior. *Nat. Neurosci.* **25**, 11–19 (2022).
133. Helmchen, F., Fee, M. S., Tank, D. W. & Denk, W. A miniature head-mounted two-photon microscope. High-resolution brain imaging in freely moving animals. *Neuron* **31**, 903–912 (2001).
134. Wallace, D. J. et al. Rats maintain an overhead binocular field at the expense of constant fusion. *Nature* **498**, 65–69 (2013).
135. Obenhaus, H. A. et al. Functional network topography of the medial entorhinal cortex. *Proc. Natl Acad. Sci. USA* **119**, e2121655119 (2022).
136. Dombeck, D. A., Harvey, C. D., Tian, L., Looger, L. L. & Tank, D. W. Functional imaging of hippocampal place cells at cellular resolution during virtual navigation. *Nat. Neurosci.* **13**, 1433–1440 (2010).
137. Morcos, A. S. & Harvey, C. D. History-dependent variability in population dynamics during evidence accumulation in cortex. *Nat. Neurosci.* **19**, 1672–1681 (2016).
138. Tuncdemir, S. N. et al. Parallel processing of sensory cue and spatial information in the dentate gyrus. *Cell Rep.* **38**, 110257 (2022).
139. Poort, J. et al. Learning and attention increase visual response selectivity through distinct mechanisms. *Neuron* **110**, 686–697 e686 (2022).
140. Khan, A. G. et al. Distinct learning-induced changes in stimulus selectivity and interactions of GABAergic interneuron classes in visual cortex. *Nat. Neurosci.* **21**, 851–859 (2018).
141. Poort, J. et al. Learning enhances sensory and multiple non-sensory representations in primary visual cortex. *Neuron* **86**, 1478–1490 (2015).
142. Grienberger, C. & Magee, J. C. Entorhinal cortex directs learning-related changes in CA1 representations. Preprint at *bioRxiv* https://doi.org/10.1101/2021.12.10.472158 (2021).
143. Tervo, D. G. et al. A designer AAV variant permits efficient retrograde access to projection neurons. *Neuron* **92**, 372–382 (2016).
144. Goel, A. et al. Impaired perceptual learning in a mouse model of Fragile X syndrome is mediated

by parvalbumin neuron dysfunction and is reversible. *Nat. Neurosci.* **21**, 1404–1411 (2018).
145. de Vries, S. E. J. et al. A large-scale standardized physiological survey reveals functional organization of the mouse visual cortex. *Nat. Neurosci.* **23**, 138–151 (2020).
146. Steinmetz, N. A. et al. Neuropixels 2.0: a miniaturized high-density probe for stable, long-term brain recordings. *Science* **372**, eabf4588 (2021).
147. Bajar, B. T. et al. A discrete neuronal population coordinates brain-wide developmental activity. *Nature* **602**, 639–646 (2022).
148. Park, J. E. et al. Generation of transgenic marmosets expressing genetically encoded calcium indicators. *Sci. Rep.* **6**, 34931 (2016).
149. Katlowitz, K. A., Picardo, M. A. & Long, M. A. Stable sequential activity underlying the maintenance of a precisely executed skilled behavior. *Neuron* **98**, 1133–1140.e3 (2018).
150. Xie, Y. et al. Geometry of sequence working memory in macaque prefrontal cortex. *Science* **375**, 632–639 (2022).
151. Trautmann, E. M. et al. Dendritic calcium signals in rhesus macaque motor cortex drive an optical brain–computer interface. *Nat. Commun.* **12**, 3689 (2021).
152. Petreanu, L., Huber, D., Sobczyk, A. & Svoboda, K. Channelrhodopsin-2-assisted circuit mapping of long-range callosal projections. *Nat. Neurosci.* **10**, 663–668 (2007).
153. Cossart, R., Aronov, D. & Yuste, R. Attractor dynamics of network UP states in the neocortex. *Nature* **423**, 283–288 (2003).
154. Ikegaya, Y. et al. Synfire chains and cortical songs: temporal modules of cortical activity. *Science* **304**, 559–564 (2004).
155. Motanis, H. & Buonomano, D. Decreased reproducibility and abnormal experience-dependent plasticity of network dynamics in Fragile X circuits. *Sci. Rep.* **10**, 14535 (2020).
156. Samarasinghe, R. A. et al. Identification of neural oscillations and epileptiform changes in human brain organoids. *Nat. Neurosci.* **24**, 1488–1500 (2021).
157. Buzsaki, G. Neural syntax: cell assemblies, synapsembles, and readers. *Neuron* **68**, 362–385 (2010).
158. Churchland, M. M. et al. Neural population dynamics during reaching. *Nature* **487**, 51–56 (2012).
159. Villette, V., Malvache, A., Tressard, T., Dupuy, N. & Cossart, R. Internally recurring hippocampal sequences as a population template of spatiotemporal information. *Neuron* **88**, 357–366 (2015).
160. Yuste, R. From the neuron doctrine to neural networks. *Nat. Rev. Neurosci.* **16**, 487–497 (2015).
161. Nikolenko, V. et al. SLM microscopy: scanless two-photon imaging and photostimulation with spatial light modulators. *Front. Neural Circuits* **2**, 5 (2008).
162. Rickgauer, J. P., Deisseroth, K. & Tank, D. W. Simultaneous cellular-resolution optical perturbation and imaging of place cell firing fields. *Nat. Neurosci.* **17**, 1816–1824 (2014).
163. Carrillo-Reid, L., Han, S., Yang, W., Akrouh, A. & Yuste, R. Controlling visually guided behavior by holographic recalling of cortical ensembles. *Cell* **178**, 447–457.e5 (2019).
164. Clancy, K. B., Koralek, A. C., Costa, R. M., Feldman, D. E. & Carmena, J. M. Volitional modulation of optically recorded calcium signals during neuroprosthetic learning. *Nat. Neurosci.* **17**, 807–809 (2014).
165. Cichon, J. & Gan, W. B. Branch-specific dendritic Ca²⁺ spikes cause persistent synaptic plasticity. *Nature* **520**, 180–185 (2015).
166. Harnett, M. T., Makara, J. K., Spruston, N., Kath, W. L. & Magee, J. C. Synaptic amplification by dendritic spines enhances input cooperativity. *Nature* **491**, 599–602 (2012).
167. Kerlin, A. et al. Functional clustering of dendritic activity during decision-making. *eLife* **8**, e46966 (2019).
168. Gambino, F. et al. Sensory-evoked LTP driven by dendritic plateau potentials in vivo. *Nature* **515**, 116–119 (2014).
169. Fiser, A. et al. Experience-dependent spatial expectations in mouse visual cortex. *Nat. Neurosci.* **19**, 1658–1664 (2016).
170. Penagarikano, O. et al. Absence of CNTNAP2 leads to epilepsy, neuronal migration abnormalities, and core autism-related deficits. *Cell* **147**, 235–246 (2011).
171. Goncalves, J. T., Anstey, J. E., Golshani, P. & Portera-Cailliau, C. Circuit level defects in the developing neocortex of fragile X mice. *Nat. Neurosci.* **16**, 903–909 (2013).

172. La Fata, G. et al. FMRP regulates multipolar to bipolar transition affecting neuronal migration and cortical circuitry. *Nat. Neurosci.* **17**, 1693–1700 (2014).
173. Chen, Q. et al. Dysfunction of cortical GABAergic neurons leads to sensory hyper-reactivity in a Shank3 mouse model of ASD. *Nat. Neurosci.* **23**, 520–532 (2020).
174. Busche, M. A. et al. Clusters of hyperactive neurons near amyloid plaques in a mouse model of Alzheimer's disease. *Science* **321**, 1686–1689 (2008).
175. Grienberger, C. et al. Staged decline of neuronal function in vivo in an animal model of Alzheimer's disease. *Nat. Commun.* **3**, 774 (2012).
176. Korzhova, V. et al. Long-term dynamics of aberrant neuronal activity in awake Alzheimer's disease transgenic mice. *Commun. Biol.* **4**, 1368 (2021).
177. Virani, S. S. et al. Heart disease and stroke statistics — 2021 update: a report from the American Heart Association. *Circulation* **143**, e254–e743 (2021).
178. Fordsmann, J. C. et al. Spontaneous astrocytic Ca²⁺ activity abounds in electrically suppressed ischemic penumbra of aged mice. *Glia* **67**, 37–52 (2019).
179. Shih, A. Y. et al. The smallest stroke: occlusion of one penetrating vessel leads to infarction and a cognitive deficit. *Nat. Neurosci.* **16**, 55–63 (2013).
180. Rakers, C. & Petzold, G. C. Astrocytic calcium release mediates peri-infarct depolarizations in a rodent stroke model. *J. Clin. Invest.* **127**, 511–516 (2017).
181. Murphy, T. H., Li, P., Betts, K. & Liu, R. Two-photon imaging of stroke onset in vivo reveals that NMDA-receptor independent ischemic depolarization is the major cause of rapid reversible damage to dendrites and spines. *J. Neurosci.* **28**, 1756–1772 (2008).
182. Ding, S., Wang, T., Cui, W. & Haydon, P. G. Photothrombosis ischemia stimulates a sustained astrocytic Ca²⁺ signaling in vivo. *Glia* **57**, 767–776 (2009).
183. Liu, L. et al. Microglial calcium waves during the hyperacute phase of ischemic stroke. *Stroke* **52**, 274–283 (2021).
184. Brawek, B. & Garaschuk, O. Monitoring in vivo function of cortical microglia. *Cell Calcium* **64**, 109–117 (2017).
185. Alarcon-Martinez, L. et al. Interpericyte tunnelling nanotubes regulate neurovascular coupling. *Nature* **585**, 91–95 (2020).
186. Winship, I. R. & Murphy, T. H. In vivo calcium imaging reveals functional rewiring of single somatosensory neurons after stroke. *J. Neurosci.* **28**, 6592–6606 (2008).
187. Zeiger, W. A. et al. Barrel cortex plasticity after photothrombotic stroke involves potentiating responses of pre-existing circuits but not functional remapping to new circuits. *Nat. Commun.* **12**, 3972 (2021).
188. Tennant, K. A., Taylor, S. L., White, E. R. & Brown, C. E. Optogenetic rewiring of thalamocortical circuits to restore function in the stroke injured brain. *Nat. Commun.* **8**, 15879 (2017).
189. Motaharinia, M. et al. Longitudinal functional imaging of VIP interneurons reveals sup-population specific effects of stroke that are rescued with chemogenetic therapy. *Nat. Commun.* **12**, 6112 (2021).
190. Nimmerjahn, A., Kirchhoff, F., Kerr, J. N. & Helmchen, F. Sulforhodamine 101 as a specific marker of astroglia in the neocortex in vivo. *Nat. Methods* **1**, 31–37 (2004).
191. Reeves, A. M., Shigetomi, E. & Khakh, B. S. Bulk loading of calcium indicator dyes to study astrocyte physiology: key limitations and improvements using morphological maps. *J. Neurosci.* **31**, 9353–9358 (2011).
192. Jiang, R., Haustein, M. D., Sofroniew, M. V. & Khakh, B. S. Imaging intracellular Ca²⁺ signals in striatal astrocytes from adult mice using genetically-encoded calcium indicators. *J. Vis. Exp.* https://doi.org/10.3791/51972 (2014).
193. Srinivasan, R. et al. New transgenic mouse lines for selectively targeting astrocytes and studying calcium signals in astrocyte processes in situ and in vivo. *Neuron* **92**, 1181–1195 (2016).
194. Bjornstad, D. M. et al. Begonia — a two-photon imaging analysis pipeline for astrocytic Ca²⁺ signals. *Front. Cell Neurosci.* **15**, 681066 (2021).
195. Eichhoff, G., Brawek, B. & Garaschuk, O. Microglial calcium signal acts as a rapid sensor of single neuron damage in vivo. *Biochim. Biophys. Acta* **1813**, 1014–1024 (2011).
196. Tvrdik, P. et al. Calcium imaging of microglial network activity in stroke. *Methods Mol. Biol.* **2034**, 267–279 (2019).
197. Tworig, J. M., Coate, C. J. & Feller, M. B. Excitatory neurotransmission activates compartmentalized calcium transients in Müller glia without affecting lateral process motility. *eLife* **10**, e73202 (2021).

198. Tong, L. et al. Imaging and optogenetic modulation of vascular mural cells in the live brain. *Nat. Protoc.* **16**, 472–496 (2021).
199. Hirase, H., Creso, J., Singleton, M., Bartho, P. & Buzsaki, G. Two-photon imaging of brain pericytes in vivo using dextran-conjugated dyes. *Glia* **46**, 95–100 (2004).
200. Gilbert, T. L. & Ng, L. in *Molecular-Genetic and Statistical Techniques for Behavioral and Neural Research* (ed. Gerlai, R. T.) 51–72 (Academic, 2018).
201. Sadovsky, A. J. et al. Heuristically optimal path scanning for high-speed multiphoton circuit imaging. *J. Neurophysiol.* **106**, 1591–1598 (2011).
202. Otsu, Y. et al. Optical monitoring of neuronal activity at high frame rate with a digital random-access multiphoton (RAMP) microscope. *J. Neurosci. Methods* **173**, 259–270 (2008).
203. Szalay, G. et al. Fast 3D imaging of spine, dendritic, and neuronal assemblies in behaving animals. *Neuron* **92**, 723–738 (2016).
204. Grewe, B. F., Langer, D., Kasper, H., Kampa, B. M. & Helmchen, F. High-speed in vivo calcium imaging reveals neuronal network activity with near-millisecond precision. *Nat. Methods* **7**, 399–405 (2010).
205. Chen, X., Leischner, U., Rochefort, N. L., Nelken, I. & Konnerth, A. Functional mapping of single spines in cortical neurons in vivo. *Nature* **475**, 501–505 (2011).
206. Villette, V. et al. Ultrafast two-photon imaging of a high-gain voltage indicator in awake behaving mice. *Cell* **179**, 1590–1608.e23 (2019).
207. Economo, M. N., Hansen, K. R. & Wachowiak, M. Control of mitral/tufted cell output by selective inhibition among olfactory bulb glomeruli. *Neuron* **91**, 397–411 (2016).
208. Vladimirov, N. et al. Brain-wide circuit interrogation at the cellular level guided by online analysis of neuronal function. *Nat. Methods* **15**, 1117–1125 (2018).
209. Sofroniew, N. J., Flickinger, D., King, J. & Svoboda, K. A large field of view two-photon mesoscope with subcellular resolution for in vivo imaging. *eLife* **5**, e14472 (2016).
210. Stirman, J. N., Smith, I. T., Kudenov, M. W. & Smith, S. L. Wide field-of-view, multi-region, two-photon imaging of neuronal activity in the mammalian brain. *Nat. Biotechnol.* **34**, 857–862 (2016).
211. Tsai, P. S. et al. Ultra-large field-of-view two-photon microscopy. *Opt. Express* **23**, 13833–13847 (2015).
212. Amir, W. et al. Simultaneous imaging of multiple focal planes using a two-photon scanning microscope. *Opt. Lett.* **32**, 1731–1733 (2007).
213. Yu, C. H., Stirman, J. N., Yu, Y., Hira, R. & Smith, S. L. Diesel2p mesoscope with dual independent scan engines for flexible capture of dynamics in distributed neural circuitry. *Nat. Commun.* **12**, 6639 (2021).
214. Chen, J. L., Voigt, F. F., Javadzadeh, M., Krueppel, R. & Helmchen, F. Long-range population dynamics of anatomically defined neocortical networks. *eLife* **5**, e14679 (2016).
215. Zhang, T. et al. Kilohertz two-photon brain imaging in awake mice. *Nat. Methods* **16**, 1119–1122 (2019).
216. Demas, J. et al. High-speed, cortex-wide volumetric recording of neuroactivity at cellular resolution using light beads microscopy. *Nat. Methods* **18**, 1103–1111 (2021).
217. Rumyantsev, O. I. et al. Fundamental bounds on the fidelity of sensory cortical coding. *Nature* **580**, 100–105 (2020).
218. Yang, W. & Yuste, R. In vivo imaging of neural activity. *Nat. Methods* **14**, 349–359 (2017).
219. Theer, P., Hasan, M. T. & Denk, W. Two-photon imaging to a depth of 1000 microm in living brains by use of a Ti:Al₂O₃ regenerative amplifier. *Opt. Lett.* **28**, 1022–1024 (2003).
220. Ebina, T. et al. Two-photon imaging of neuronal activity in motor cortex of marmosets during upper-limb movement tasks. *Nat. Commun.* **9**, 1879 (2018).
221. Sherman, L., Ye, J. Y., Albert, O. & Norris, T. B. Adaptive correction of depth-induced aberrations in multiphoton scanning microscopy using a deformable mirror. *J. Microsc.* **206**, 65–71 (2002).
222. Ji, N., Milkie, D. E. & Betzig, E. Adaptive optics via pupil segmentation for high-resolution imaging in biological tissues. *Nat. Methods* **7**, 141–147 (2010).
223. Wang, C. et al. Multiplexed aberration measurement for deep tissue imaging in vivo. *Nat. Methods* **11**, 1037–1040 (2014).
224. Girkin, J. M., Poland, S. & Wright, A. J. Adaptive optics for deeper imaging of biological samples. *Curr. Opin. Biotechnol.* **20**, 106–110 (2009).
225. Sun, W., Tan, Z., Mensh, B. D. & Ji, N. Thalamus provides layer 4 of primary visual cortex with orientation- and direction-tuned inputs. *Nat. Neurosci.* **19**, 308–315 (2016).
226. Mittmann, W. et al. Two-photon calcium imaging of evoked activity from L5 somatosensory neurons in vivo. *Nat. Neurosci.* **14**, 1089–1093 (2011).
227. Wang, T. et al. Three-photon imaging of mouse brain structure and function through the intact skull. *Nat. Methods* **15**, 789–792 (2018).
228. Horton, N. G. et al. In vivo three-photon microscopy of subcortical structures within an intact mouse brain. *Nat. Photonics* **7**, 205–209 (2013).
229. Ouzounov, D. G. et al. In vivo three-photon imaging of activity of GCaMP6-labeled neurons deep in intact mouse brain. *Nat. Methods* **14**, 388–390 (2017).
230. Streich, L. et al. High-resolution structural and functional deep brain imaging using adaptive optics three-photon microscopy. *Nat. Methods* **18**, 1253–1258 (2021).
231. Weisenburger, S. et al. Volumetric Ca²⁺ imaging in the mouse brain using hybrid multiplexed sculpted light microscopy. *Cell* **177**, 1050–1066.e14 (2019).
232. Zong, W. et al. Large-scale two-photon calcium imaging in freely moving mice. *Cell* **185**, 1240–1256.e30 (2022).
233. Paninski, L. & Cunningham, J. P. Neural data science: accelerating the experiment–analysis–theory cycle in large-scale neuroscience. *Curr. Opin. Neurobiol.* **50**, 232–241 (2018).
234. Giovannucci, A., et al. in *Advances in Neural Information Processing Systems* (NIPS, 2017).
235. Zhang, Z., Russell, L. E., Packer, A. M., Gauld, O. M. & Hausser, M. Closed-loop all-optical interrogation of neural circuits in vivo. *Nat. Methods* **15**, 1037–1040 (2018).
236. O'Shea, D. J. et al. The need for calcium imaging in nonhuman primates: new motor neuroscience and brain–machine interfaces. *Exp. Neurol.* **287**, 437–451 (2017).
237. Abdelfattah, A. S. et al. Bright and photostable chemigenetic indicators for extended in vivo voltage imaging. *Science* **365**, 699–704 (2019).
238. Chien, M. P. et al. Photoactivated voltage imaging in tissue with an archaerhodopsin-derived reporter. *Sci. Adv.* **7**, eabe3216 (2021).
239. Gong, Y. et al. High-speed recording of neural spikes in awake mice and flies with a fluorescent voltage sensor. *Science* **350**, 1361–1366 (2015).
240. Piatkevich, K. D. et al. Population imaging of neural activity in awake behaving mice. *Nature* **574**, 413–417 (2019).
241. Marvin, J. S. et al. Stability, affinity, and chromatic variants of the glutamate sensor iGluSnFR. *Nat. Methods* **15**, 936–939 (2018).
242. Patriarchi, T. et al. Ultrafast neuronal imaging of dopamine dynamics with designed genetically encoded sensors. *Science* **360**, eaat4422 (2018).
243. Ji, N., Freeman, J. & Smith, S. L. Technologies for imaging neural activity in large volumes. *Nat. Neurosci.* **19**, 1154–1164 (2016).
244. Charles, A. S. et al. Toward community-driven big open brain science: open big data and tools for structure, function, and genetics. *Annu. Rev. Neurosci.* **43**, 441–464 (2020).
245. Emiliani, V., Cohen, A. E., Deisseroth, K. & Hausser, M. All-optical interrogation of neural circuits. *J. Neurosci.* **35**, 13917–13926 (2015).
246. Cai, C., Dong, C., Rozsa, B., Pnevmatikakis, E. & Giovannucci, A. FIOLA: an accelerated pipeline for Fluorescence Imaging OnLine Analysis. Preprint at *Res. Sq.* https://doi.org/10.21203/rs.3.rs-800247/v1 (2021).
247. Adesnik, H. & Abdeladim, L. Probing neural codes with two-photon holographic optogenetics. *Nat. Neurosci.* **24**, 1356–1366 (2021).
248. Picardo, M. A. et al. Population-level representation of a temporal sequence underlying song production in the zebra finch. *Neuron* **90**, 866–876 (2016).
249. Jun, J. J. et al. Fully integrated silicon probes for high-density recording of neural activity. *Nature* **551**, 232–236 (2017).
250. Steinmetz, N. A., Koch, C., Harris, K. D. & Carandini, M. Challenges and opportunities for large-scale electrophysiology with Neuropixels probes. *Curr. Opin. Neurobiol.* **50**, 92–100 (2018).
251. Lima, S. Q., Hromadka, T., Znamenskiy, P. & Zador, A. M. PINP: a new method of tagging neuronal populations for identification during in vivo electrophysiological recording. *PLoS ONE* **4**, e6099 (2009).
252. Vollmer, K. M. et al. A novel assay allowing drug self-administration, extinction, and reinstatement testing in head-restrained mice. *Front. Behav. Neurosci.* **15**, 744715 (2021).
253. Seidemann, E. et al. Calcium imaging with genetically encoded indicators in behaving primates. *eLife* **5**, e16178 (2016).
254. Wilt, B. A., Fitzgerald, J. E. & Schnitzer, M. J. Photon shot noise limits on optical detection of neuronal spikes and estimation of spike timing. *Biophys. J.* **104**, 51–62 (2013).
255. Anderson, M. A. et al. Astrocyte scar formation aids central nervous system axon regeneration. *Nature* **532**, 195–200 (2016).
256. Sheffield, M. E. & Dombeck, D. A. Calcium transient prevalence across the dendritic arbour predicts place field properties. *Nature* **517**, 200–204 (2015).
257. Theriault, G., Cottet, M., Castonguay, A., McCarthy, N. & De Koninck, Y. Extended two-photon microscopy in live samples with Bessel beams: steadier focus, faster volume scans, and simpler stereoscopic imaging. *Front. Cell Neurosci.* **8**, 139 (2014).
258. Lu, R. et al. Video-rate volumetric functional imaging of the brain at synaptic resolution. *Nat. Neurosci.* **20**, 620–628 (2017).
259. Song, A. et al. Volumetric two-photon imaging of neurons using stereoscopy (vTwINS). *Nat. Methods* **14**, 420–426 (2017).
260. Prevedel, R. et al. Fast volumetric calcium imaging across multiple cortical layers using sculpted light. *Nat. Methods* **13**, 1021–1028 (2016).

Supplementary information
The online version contains supplementary material available at https://doi.org/10.1038/s43586-022-00147-1.

RELATED LINKS
Allen Brain Observatory: https://observatory.brain-map.org/visualcoding/
CRCNS: https://crcns.org/
DANDI: https://www.dandiarchive.org/
DataJoint: https://www.datajoint.org/
FigShare: https://figshare.com/
IARPA MICrONS: https://www.iarpa.gov/research-programs/microns
International Brain Laboratory: https://www.internationalbrainlab.com/
NeuroCAAS: http://www.neurocaas.org/
NWB: https://www.nwb.org/
Zenodo: https://zenodo.org/